1. Materials and methods

General

General instrumentation (MS, HPLC, small-animal PET) and procedures (determination of IC_{50} in cell assays, automated ^{68}Ga-labelling, animal models and handling, PET imaging and data processing) have been described recently.[1,2] However, important protocols and procedures are repeated herein for convenience.

TRAP and TRAP(CHX)$_3$,[3] as well as TRAP(alkyne)$_3$,[4] were prepared as described previously. DUPA-Pep was obtained from ABX (Radeberg, Germany). 5-Azidopentanoic acid was purchased from Sigma-Aldrich. 3-Azidopropylamine was purchased from Alfa Aesar. DOTAGA-anhydride was obtained from CheMatech (Dijon, France).

TRAP(azide)$_3$

TRAP(azide)$_3$ was prepared according to a previously published proecure.[4] TRAP (500 mg, 0.8 mmol, 1 eq.), DIPEA (2.07 mL, 12 mmol, 15 eq.) and 3-azido-prop-1-ylamin (400 mg, 4 mmol, 5 eq.) were dissolved in dry DMSO (5 mL). Then HATU (2.4 mg, 6.5 mmol, 8 eq.) was added in small portions during 15 min. After stirring for additional 15 min, the reaction mixture was diluted with water (50 mL) and concentrated to 15 mL by ultrafiltration (Amicon®/Millipore setup, consisting of a 50 mL stirred cell and a 800 mL mini-reservoir, using a cellulose acetate membrane, filter code YC05, with 500 Da MWCO). Diafiltration (continuous ultrafiltration) with 0.05 M aq. NaCl (200 mL) and water (100 mL) removed most of the impurities (coupling reagents and remains thereof). After lyophilisation, a final purification was done by HPLC (YMC ODS-H80 RP column, 150×20 mm; flow 10 mL/min; gradient 5–50% MeCN in water, both containing 0.1% trifluoroacetic acid, within 10 min; UV detection at 220 nm; t_R =9.5 min). Lyophilisation yielded 370 mg of TRAP(azide)$_3$ as a colorless solid.

^{1}H-NMR (500 MHz, D_2O, 300 K): δ = 1.72 (p, 6H, $^3J_{HH}$ = 6.7 Hz, CH_2–C*H*$_2$–CH_2), 1.90–1.96 (m, 6H, C(O)–C*H*$_2$), 2.39–2.45 (m, 6H, P–C*H*$_2$–C), 3.21 (t, $^3J_{HH}$ = 6.7 Hz, 6H, P–C*H*$_2$–N), 3.29–3.34 (m, 12H, C(O)–NH–C*H*$_2$ and N_3–C*H*$_2$), 3.38 (s, 12H, ring-C*H*$_2$) ppm. ^{13}C-NMR (125 MHz, D_2O, 300 K): δ = 25.6 (P–*C*–C, $^1J_{PC}$ = 93 Hz), 27.5 (C(O)–*C*), 27.8 (C–*C*–C), 36.7 (N_3–*C*), 48.5 (ring-*C*), 51.3 (C(O)–O–*C*), 54.0 (P–*C*–N, $^1J_{PC}$ = 92 Hz), 174.6 (*C*(O), $^3J_{PP}$ = 14 Hz) ppm. ^{31}P-NMR (202 MHz, D_2O, 300 K): δ = 38.9. MS (ESI, positive): *m*/*z* = 826 $[M+H^+]^+$, 848 $[M+Na^+]^+$

DOTAGA-DUPA-Pep

To a solution of DUPA-Pep (10 mg, 12.5 µmol, 1 eq) in DMF (0.75 mL), DOTAGA-anhydride (5.7 mg, 12.5 µmol, 1 eq) and triethylamine (5.2 µL, 37.5 µmol, 3 eq) were added and stirred at 70 °C for 2 h. The product was precipitated by dropwise addition of the reaction mixture to diethylether and purified by HPLC (Multospher 100 RP18-5 µm column, 250×20 mm; flow 9 mL/min; gradient 25–55% MeCN in water, both containing 0.1% trifluoroacetic acid, within 24 min; UV detection at 220 nm). After evaporation of organic components and lyophilization, 1.8 mg of DOTAGA-DUPA-Pep were obtained in form of a colorless solid MW: 1255.6; MS (ESI positive): *m/z* = 1256.4 $[M+H]^+$, 1278.4 $[M+Na]^+$, 628.7 $[M+2H]^{2+}$

DUPA-Pep-azide

HATU (5.2 mg, 13.8 µmol, 1.1 eq.) was added to a solution of 5-azidopentanoic acid (2.5 mg, 17.5 µmol, 1.4 eq.) and DIPEA (20 µL, 15.1 mg, 117 µmol, 9.4 eq.) in DMF (100 µL). The resulting yellow solution was stirred for 10 minutes at room temperature, and subsequently added dropwise to a stirred solution of DUPA-Pep (10 mg, 12.5 µmol, 1.0 eq.) and DIPEA (14 µL, 10.6 mg, 82.0 µmol, 6.5 eq.) in DMF (200 µL). This mixture was stirred for another 60 min at r.t., and the crude product precipitated by dropwise addition to diethyl ether (25 mL). The solid was centrifuged off and purified by preparative HPLC (Multospher 100 RP18-5 µm column, 250×20 mm; flow 9 mL/min; gradient 37–41% MeCN in water, both containing 0.1% trifluoroacetic acid, within 20 min; UV detection at 220 nm; t_R = 16 min). After evaporation of organic components and lyophilization, DUPA-Pep-azide (4.20 mg, 4.55 µmol, 36 %) was obtained as a colorless solid. MW: 923.02. MS (ESI positive): *m/z* = 923.6 [*M*+H^+].

TRAP(DUPA-Pep)$_3$

TRAP(alkyne)$_3$ (6.8 mg, 9.0 µmol, 1.0 eq.), sodium ascorbate (17.9 mg, 90.0 µmol, 10 eq.) and DUPA-Pep-azide (27.3 mg, 29.5 µmol, 3.3 eq.) were dissolved in water (200 µL). After addition of a solution of $Cu(OAc)_2$ (2.15 mg, 10.7 µmol, 1.2 eq.) in water (90 µL), the reaction mixture was stirred for 1 hour. Reaction control was done by HPLC (Nucleosil 100 C18-5 µm column, 125×4 mm; flow 1 mL/min; gradient 10–50% MeCN in water, both containing 0.1% trifluoroacetic acid, within 16 min; UV detection at 220 nm) and showed complete disappearance of the signal for TRAP(alkyne)$_3$ after 30 min. In addition, only the fully functionalized product, Cu(TRAP(DUPA-Pep)$_3$) and small remains of DUPA-Pep-azide

were detected. Then, 1,4,7-triazacyclononane-*N,N′,N″*-triacetic acid trihydrochloride (NOTA·3HCl, 44 mg, 90 µmol, 10 eq.) and methanol (1 mL) were added. The pH value (tested with Merck Acilit® pH paper) was approx. 3. After standing at room temperature for three days, the solution was directly subjected to HPLC purification (Multospher 100 RP18-5 µm column, 250×20 mm; flow 9 mL/min; gradient 39–45% MeCN in water, both containing 0.1% trifluoroacetic acid, within 20 min; UV detection at 220 nm). Evaporation of organic solvent in vacuo and lyophilisation of the aqueous residue yielded TRAP(DUPA-Pep)$_3$ (9.4 mg, approx. 30%) in form of a colorless solid. MW: 3459.7. MS (ESI positive): m/z = 1730.8 [M+2H$^+$], 1154.0 [M+3H$^+$]

Cell culture

PSMA$^+$ LNCaP cells (CLS**:** 300265) were grown in Dulbecco's modified Eagle medium/Nutrition Mix F-12 with Glutamax-I (1:1) (Invitrogen, Life Technologies, Darmstadt, Germany) supplemented with 10% FCS at 37 °C in a 5% CO_2/humidified air atmosphere. Cells were harvested using Trypsin/EDTA (0.05% and 0.02%) in PBS, centrifuged and resuspended with culture medium. For cell counting, a Countesse automated cell counter (Invitrogen, Carlsbad, USA) was used. For IC_{50} determination, 150,000 cells/mL were transferred to 24-well plates (1 mL/well) one day prior to the experiment.

Determination of IC_{50}

Non-radioactive Ga^{III} complexes of DOTAGA-DUPA-Pep and TRAP(DUPA-Pep)$_3$ were prepared by adding 2 mM gallium nitrate (0.5 mL) to the same volume of a 2 mM solution of the respective chelator conjugate. Complete complex formation occured immediately and was confirmed by ESI-MS.

The culture medium was removed and the cells were washed once with 500 µL of HBSS (Hank's balanced salt solution, Biochrom, Berlin, Germany, containing 1% bovine serum albumin (BSA)), before being left to equilibrate in 200 µL of HBSS (1% BSA) on ice for 15 min. Then, 25 µL/well of either HBSS (1% BSA; Control), or solutions containing the non-radioactive complexes Ga-DOTAGA-DUPA-Pep or Ga-TRAP(DUPA-Pep)$_3$ in increasing concentrations (10^{-10}–10^{-4} M in HBSS (1% BSA)) were added, followed by the addition of 25 µl of ([^{125}I]I-BA)KuE in HBSS (1% BSA). Experiments were carried out in triplicate for each concentration. The final radioligand concentration was 0.2 nM in all binding assays.

Cells were incubated on ice for 60 min. Incubation was terminated by removal of the incubation medium. Cells were thoroughly rinsed with 250 µL of HBSS. The wash medium

was combined with the supernatant of the previous step. This fraction represents the amount of free radioligand. Cells were then lysed using 250 µL of 1 M NaOH, the lysate was transferred to vials and combined with 250 µL of HBSS used for rinsing the wells. Quantification of the amount of free and bound activity was performed in a γ-counter. Data were fitted using GraphPad Prism software.

Automated ^{68}Ga labelling

^{68}Ga labeling was performed within 15 min as described,[5] using a GallElut^{+} system (Scintomics GmbH, Germany). A ^{68}Ge/^{68}Ga-generator with SnO_2 matrix (obtained from iThemba LABS, South Africa) was eluted with 1.0 M aq. HCl. A fraction of 1.25 mL, containing approx. 80 % of the entire activity (250 MBq), was transferred into a 5 mL glass vial (Alltech, 5 mL) containing an aq. solution of HEPES (14 g in 12 mL water) and the precursor (2.5 nmol TRAP(DUPA-Pep)$_3$ with 450 µL HEPES solution, resulting in pH 2; 5 nmol DOTAGA-DUPA-Pep with 800 µL HEPES solution, resulting in pH 3). Labelling was performed for 5 min at 95 °C, followed by fixation of the peptides on pre-conditioned SPE cartridge (Waters SepPak® C8 light, purged with 10 mL of ethanol and 10 mL of water). After purging the cartridge with 10 mL of water, the labeled product was eluted by purging the cartridge with a 1:1 mixture of ethanol and water (2 mL), PBS buffer (1 mL) and again with water (1 mL). The eluate was concentrated in vacuo to 1 mL, thus leaving no ethanol in the mixture and the formulation possessing appropriate pH and osmolality for injection.

Animal model

All animal experiments were conducted in accordance with German Animal Welfare Act (Deutsches Tierschutzgesetz, approval #55.2-1-54-2532-71-13). The prostate cancer cell line LNCaP was suspended 1/1 in serum-free medium and Matrigel (BD Biosciences, Germany) and approximately 10^7 cells in 200 µL were inoculated subcutaneously on the right shoulder of 6–8 weeks old CD-1 nu/nu mice (Charles River Laboratories). Tumours were grown for 2–4 weeks (males) and 4–6 weeks (females) to reach 4–8 mm in diameter.

µPET imaging

Imaging studies were performed at a Siemens Inveon small animal PET, followed by data analysis using the Inveon Research Workplace software. The animals were anesthesized with isoflurane and injected via tail vein with approx. 12 MBq of ^{68}Ga-DOTAGA-DUPA-Pep or ^{68}Ga-TRAP(DUPA-Pep)$_3$, equivalent to 0.3 and 0.15 nmol, respectively. PET data were

recorded 60 min p.i. with an acquisition time of 15 min. Images were reconstructed using 3D ordered-subsets expectation maximum (OSEM3D) algorithm without scanner and attenuation correction.

Equilibrium studies (protonation and stability constants)

The chemicals used for the experiments were of the highest analytical grade. $CaCl_2$, $ZnCl_2$ and $CuCl_2$ solutions were prepared from solid MCl_2 (*Aldrich*; 99.9%). Concentration of $CaCl_2$, $ZnCl_2$ and $CuCl_2$ solutions were determined by complexometric titration with standardized Na_2H_2EDTA and xylenol orange ($ZnCl_2$), murexid ($CuCl_2$) and *Patton & Reeder* as indicator. The concentration of the TRAP(CHX), H_3TRAP-Pr, H_3NOTA and Na_2H_2EDTA was determined by pH-potentiometric titration in the presence and absence of a large (40-fold) excess of $CaCl_2$.

For pH measurements and titrations, a *Metrohm 785 DMP Titrino* titration workstation and a *Metrohm-6.0233.100* combined electrode were used. Equilibrium measurements were carried out at a constant ionic strength (0.15 M NaCl) in 6 mL samples at 25 °C. The solutions were stirred, and constantly purged with N_2. The titrations were performed in a pH range of 1.7–11.7. KH-phthalate (pH=4.005) and borax (pH=9.177) buffers were used to calibrate the pH meter. For calculation of $[H^+]$ from measured pH values, the method proposed by Irving et al. was used.[6] A 0.01 M HCl solution was titrated with the standardized NaOH solution in the presence of 0.1 M NaCl. Differences between the measured (pH_{read}) and calculated pH ($-\log[H^+]$) values were used to obtain the equilibrium H^+ concentration from the pH values, measured in the titration experiments.

Stability constants of Cu(TRAP(CHX)$_3$), Cu(TRAP), Cu(NOTA) and Cu(EDTA) complexes were determined by spectrophotometry, studying the Cu^{II}-TRAP(CHX)$_3$, Cu^{II}-TRAP, Cu^{II}-NOTA and Cu^{II}-EDTA systems at the absorption band of Cu^{II}-complexes at $[H^+]$ = 0.01–1.0 M over the wavelength range of 400–800 nm. Concentrations of Cu^{II}, TRAP(CHX)$_3$, TRAP, NOTA and EDTA were 3 mM. The H^+ concentration in the samples was adjusted by addition of calculated amounts of 2.0 M HCl, while ionic strength was not constant in these samples. Samples were kept at 25 °C for a week. Absorbance values were determined at 11 wavelengths (575, 595, 615, 635, 655, 675, 695, 715, 735, 755, and 775 nm). For calculation of stability and protonation constants of Cu(TRAP(CHX)$_3$), Cu(TRAP), Cu(NOTA) and Cu(EDTA), molar absorptivities of $CuCl_2$, and Cu(H_xL) species (wherein for TRAP(CHX)$_3$: x = 0, 1; TRAP: x = 0, 1, 2, 3, 4; NOTA: x = 0, 1; EDTA: x = 0, 1, 2) were determined by recording the spectra of 1.5×10^{-3}, 3.0×10^{-3} and 4.5×10^{-3} M solutions of $CuCl_2$,

Cu(TRAP(CHX)$_3$), Cu(TRAP), Cu(NOTA) and Cu(EDTA) in the pH range of 1.7–11.7. The protonation constants of Cu(TRAP(CHX)$_3$), Cu(TRAP-Pr), Cu(NOTA) and Cu(EDTA) complexes were also determined by pH-potentiometric titrations at 1:1 metal to ligand molar ratio. Calculations were done with the program PSEQUAD.[7]

Kinetic studies

The rates of the ligand exchange reactions of Cu(TRAP-Pr) and Cu(TRAP(CHX)) with NOTA and EDTA ligand were studied by following the formation of Cu(NOTA) and Cu(EDTA) complexes by spectrophotometry at 263 and 243 nm, respectively, in the pH range 1.5–4.0, in the presence of the 10, 20 and 30 fold excess of NOTA and 10 and 20 fold excess of EDTA in order to maintain pseudo-first order kinetic conditions. Concentrations of Cu(TRAP) and Cu(TRAP(CHX)$_3$) were 0.2 mM. Kinetic studies were performed with *Cary 1E* and *Cary 100 Bio* spectrophotometers, using cell holders thermostated to 15, 25, 37, and 50 °C. The pre-thermostated solutions were mixed in tandem cells (l=0.874 cm). The ionic strength of the solutions was kept constant at 0.15 M with NaCl. In order to keep the pH values constant, dichloro-acetic acid (DCA) (pH range 1.5 – 2.5), chloro-acetic acid (MCA) (pH range 2.5 – 3.5) and 1,4-dimethylpiperazine (DMP) (pH=3.1 – 4.1) buffers (0.01 M) were used. Pseudo-first-order rate constants (k_d) were calculated by fitting the absorbance values to the equation

$$A_t = (A_0 - A_e)e^{(-k_d t)} + A_e$$

wherein A_0, A_e and A_t are the absorbance values at the start, at equilibrium and at the time t of the reaction, respectively. During reactions with EDTA, the rate constants were calculated from the absorbance–time data pairs until 40–60% conversion, since the exchange does not proceed to completeness. In this case, the A_e values were calculated from the absorbance values of 0.2 mM Cu(EDTA) solution obtained at 243 nm in the pH range 1.5–4.0. The calculation of the kinetic parameters were performed by the fitting of the absorbance–time data pairs with the *Micromath Scientist* computer program (version 2.0, Salt Lake City, UT, USA).

NMR measurements

^{1}H-NMR spectra of the Zn^{II}-NOTA and ^{31}P-NMR spectra of Zn^{II}-TRAP(CHX)$_3$ and Zn^{II}-TRAP-Pr were recorded by using a Bruker DRX 400 NMR (9.4 T) spectrometer, equipped with a Bruker VT-1000 thermocontroller and a 5 mm broad band probe head. 10 mM Zn^{II}-

NOTA, Zn^{II}-TRAP$(CHX)_3$ and Zn^{II}-TRAP solutions were prepared in H_2O, while D_2O was added as an external standard in an inset tube. H^+ concentrations in the samples were adjusted by addition of calculated amounts of 2.0 M HCl, while ionic strength was not constant in these samples. Chemical shifts are reported in ppm with respect to DSS (4,4-dimethyl-4-silapentane-1-sulfonic acid) for ^1H and H_3PO_4 for ^{31}P, as external standards (0 ppm). ^{31}P-NMR spectra of Zn^{II}-TRAP$(CHX)_3$ and Zn^{II}-TRAP systems were recorded in selective ^1H decoupling mode, operating with 40 dB attenuated decoupling power. The spectra were analyzed with the *Bruker WinNMR* software package.

2. Protonation and complexation equilibria of TRAP, TRAP(CHX)$_3$, NOTA and EDTA ligands

The protonation equilibria of the TRAP, TRAP(CHX)$_3$, NOTA and EDTA ligands have been studied by pH-potentiometry. The protonation constants ($\log K_i^H$) of ligands are defined according to Eq. (1).

$$K_i^H = \frac{[H_i L]}{[H_{i-1}][H^+]} \qquad \text{i=0, 1, 2…6} \qquad (1)$$

The stability and protonation constants of TRAP, TRAP(CHX)$_3$ and NOTA complexes with several metal ions were investigated by pH-potentiometric, UV/Vis spectrophotometric, ^{1}H- and ^{31}P-NMR spectroscopy methods. The stability and protonation constants of the metal complexes formed with the TRAP, TRAP(CHX)$_3$ and NOTA ligands, defined by Eqs. (2) and (3), are listed in Table S1:

$$K_{ML} = \frac{[ML]}{[M][L]} \qquad (2)$$

$$K_{MH_iL} = \frac{[MH_iL]}{[MH_{i-1}L][H^+]} \qquad (3)$$

where i = 1, 2, 3. The K_{ML} and K_{MHiL} values characterizing the formation of TRAP, TRAP(CHX)$_3$ and NOTA complexes of Ca^{II} and Zn^{II} have been calculated from the pH-potentiometric titration data obtained at 1:1 metal to ligand concentration ratios. pH-potentiometric titrations of TRAP ligand were also performed at 2:1 metal-to-ligand ratio in order to examine the possible formation of homo- and heterodinuclear Ca^{II}-, Zn^{II}-, and Cu^{II}-TRAP complexes. The stability and protonation constants of the homo- and heterodinuclear complexes formed with the TRAP ligand, defined by Eqs. (4)–(7), are listed in Table S2.

$$K_{M_2L} = \frac{[M_2L]}{[ML][M]} \qquad (4)$$

$$K_{M_2LH} = \frac{[M_2LH]}{[M_2L][H^+]} \qquad (5)$$

$$K_{M^*(ML)} = \frac{[M^*(ML)]}{[ML][M^*]} \qquad (6)$$

$$K_{M*(MHL)} = \frac{[M*(MHL)]}{[M*(ML)][H^+]} \qquad (7)$$

In calculating the equilibrium constants, the best fit of NaOH volume to pH data was obtained by assuming the formation of ML, MHL, MH_2L, MH_3L, MH_4L, M_2L, M_2LH, M*(ML) and M*(MHL) complexes with TRAP, TRAP$(CHX)_3$ and NOTA. The stability and protonation constants of Zn^{II}-complexes formed with TRAP, TRAP$(CHX)_3$ and NOTA have also been determined by ^{1}H- and ^{31}P-NMR spectroscopy. The equilibrium reaction (8) has been studied in the $[H^+]$ range of 0.01–0.32 M, where the formation of Zn^{II}, $Zn(H_xL)$ and H_yL species was assumed (TRAP$(CHX)_3$: x = 0; y = 2, 3; TRAP: x = 3, 4; y = 5, 6; NOTA: x = 0, 1; y = 3, 4).

$$Zn^{II} + H_yL \rightleftharpoons [Zn(H_xL)] + y\text{-}xH^+ \qquad (8)$$

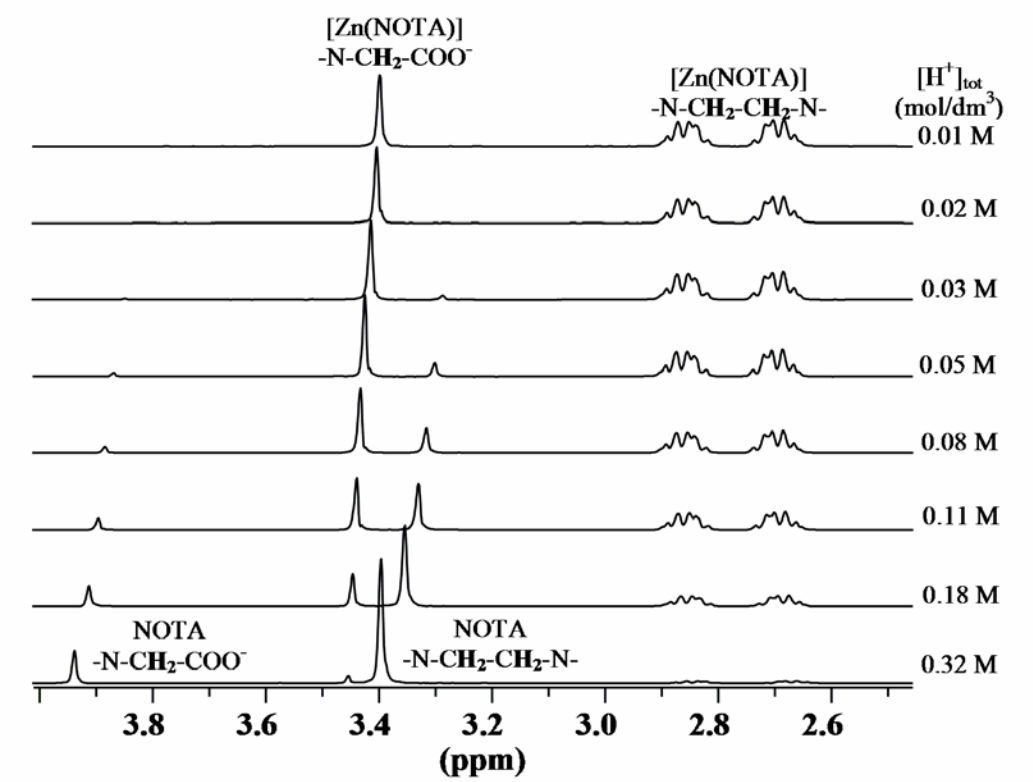

Figure S1: ^{1}H-NMR spectra of Zn^{II}-NOTA systems ($[Zn^{II}]$=[NOTA]=0.01 M, $[H^+]+[Na^+]$=0.15 M in the last 6 samples, 298 K)

The ^{1}H-NMR spectra of Zn^{II}-NOTA and ^{31}P-NMR spectra of Zn^{II}-TRAP systems are shown in Figures S1 and S2. (Because of the similarities of Zn^{II}-TRAP$(CHX)_3$ and Zn^{II}-TRAP systems, only the ^{31}P-NMR spectra of Zn^{II}-TRAP system are presented and discussed).

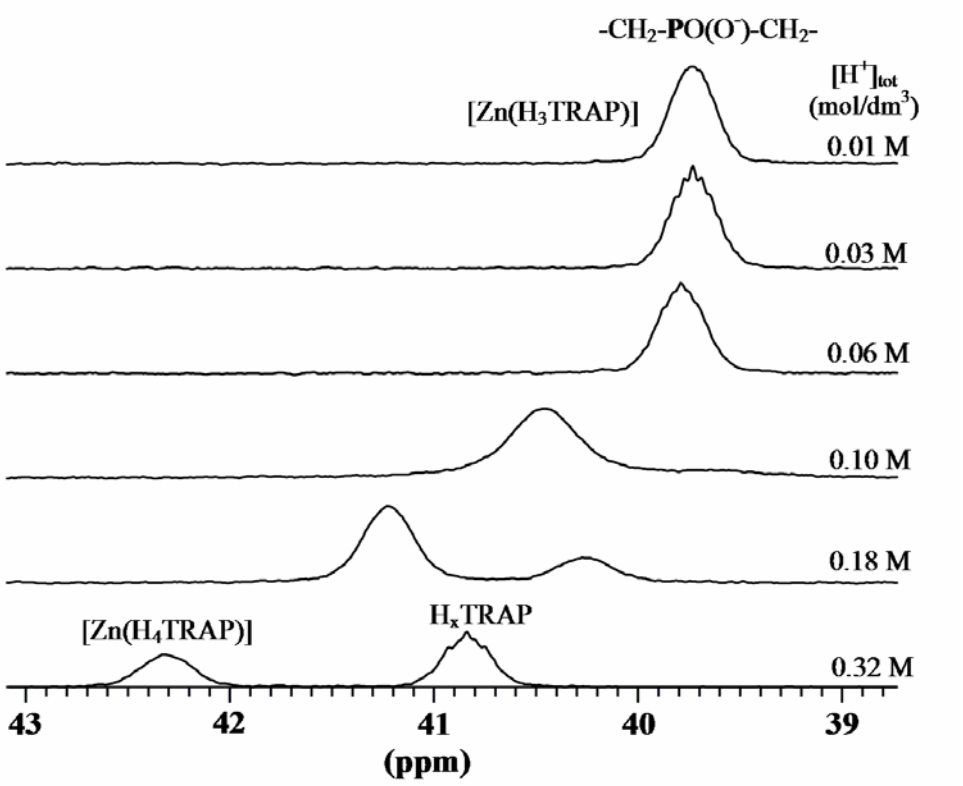

Figure S2: ^{31}P-NMR spectra of the Zn^{II}-TRAP systems ([Zn^{II}]=[TRAP]=0.01 M, [H^+]+[Na^+]=0.15 M in the last 2 samples, 298 K)

Figure S1 shows that the ^{1}H-NMR spectra of Zn^{II}-NOTA systems contain two sets of signals, which are related to protonated [Zn(HNOTA)] and H_xNOTA, indicating a slow exchange between free and complexed NOTA ligands at [H^+] = 0.32 M. In the [H^+] range 0.03–0.32 M, intensity and chemical shifts of the methylene proton signals of the free H_xNOTA ligand decreases with decrease of [H^+], due to the formation of [Zn(HNOTA)] complex and deprotonation of the free H_xNOTA ligand. At [H^+] < 0.03 M, the ^{1}H-NMR spectrum contains one set of signals which is related to the methylene protons of the [Zn(HNOTA)] complex. In the [H^+] range 0.02–0.32 M, deprotonation of [Zn(HNOTA)] results in a slight upfield shift of the ^{1}H-NMR signals of the acetate methylene protons, which indicates that protonation of [Zn(NOTA)] probably occurs at one of the carboxylate groups of the ligand. ^{1}H-NMR data were used for calculation of stability and protonation constants of the [Zn(NOTA)] complex. Integrals and chemical shift of the ^{1}H-NMR signals (acetate -C**H$_2$**- protons of [Zn(NOTA)] at 3.42 ppm, Figure S1) were used for calculation of logK_{ZnL} and logK_{ZnHL} values (Table S1) of [Zn(NOTA)], respectively.

In the ^{31}P-NMR spectra of the Zn^{II}-TRAP system ([H^+] = 0.32 M), there are two broad signals (40.8 and 42.3 ppm) which can be assigned to free H_xTRAP and the protonated [Zn(H_4TRAP)] complex, respectively (Figure S2). The appearance of two ^{31}P-NMR signals indicate a slow ligand exchange reaction between free and complexed TRAP ligand, as it was found in the Zn^{II}-NOTA system. In the [H^+] range 0.06–0.32 M, intensity and chemical shifts of the ^{31}P-NMR signal of free H_xTRAP ligand decreases with decrease of [H^+], due to formation of the [Zn(H_4TRAP)] complex and deprotonation of the free H_xTRAP ligand. At [H^+] < 0.06 M, the ^{31}P-NMR spectrum contains only one signal which is related to the phosphinate phosphorous atoms of the [Zn(H_3TRAP)] complex. In the [H^+] range 0.03–0.32 M, deprotonation of [Zn(H_4TRAP)] results in a slight upfield shift of the ^{31}P-NMR signals of the phosphorous atoms, which indicates that protonation of [Zn(H_3TRAP)] takes probably place at one of the phosphinate groups of the ligand. ^{31}P-NMR data were used for the calculation of the stability and protonation constants of the [Zn(H_3TRAP)] complex. Integrals and chemical shifts of ^{31}P-NMR signal of [Zn(H_3TRAP)] were used for the calculation of stability ($\log\beta_{Zn(H3TRAP\text{-}Pr)}$) and protonation constant ($\log K_{Zn(H4TRAP\text{-}Pr)}$) values of [Zn($H_3$TRAP)], respectively. By taking into account the protonation constants of the Zn(TRAP) complex ($\log K_{ZnHL}$=6.16, $\log K_{ZnH2L}$=4.62, $\log K_{ZnH3L}$=3.88, Table S1) determined by pH-potentiometry, the stability constant of Zn(TRAP) was calculated from the result of the ^{31}P-NMR data of the Zn^{II}-TRAP systems. The two values for the stability constant of [Zn(TRAP)], obtained by pH-potentiometry ($\log K_{ZnL}$=16.07(3)) and ^{31}P-NMR spectroscopy ($\log K_{ZnL}$=16.39(6)), are well in agreement (Table S1).

Stability and protonation constants of Cu^{II}-complexes formed with TRAP$(CHX)_3$, TRAP, NOTA and EDTA have been determined by spectrophotometry. The equilibrium reaction (9) has been studied in the [H^+] range of 0.03–1.0 M, where formation of Cu^{II}, CuH_xL, and H_yL species was assumed (TRAP$(CHX)_3$: x = 0, y = 2, 3; TRAP: x = 3, 4; y = 5, 6; NOTA: x = 0, 1, y = 3, 4; EDTA: x = 0, 1, 2; y = 4, 5).

$$Cu^{2+} + H_yL \rightleftharpoons [Cu(H_xL)] + y\text{-}xH^+ \qquad (9)$$

Some characteristic absorption spectra Cu^{II}-TRAP$(CHX)_3$, Cu^{II}-TRAP, Cu^{II}-NOTA and Cu^{II}-EDTA systems are shown in Figures S3–S6.

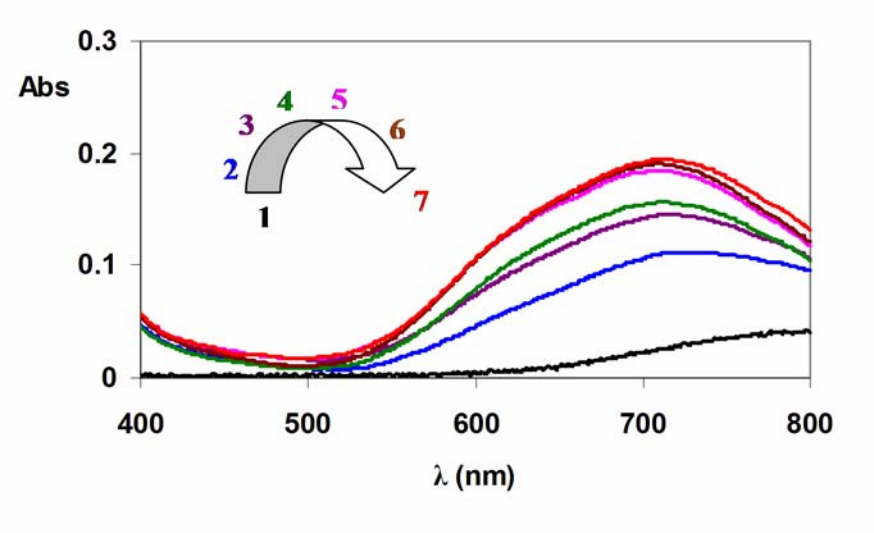

Figure S3: VIS-spectra of Cu^{II}-TRAP(CHX)$_3$ systems ([Cu^{II}]=[TRAP(CHX)$_3$]=3.0 mM, [Cu^{II}]=3.0 mM (**1**), [H^+]=1.3 M (**2**), 0.9 M (**3**), 0.6 M (**4**), 0.3 M (**5**), 0.1 M (**6**) and 0.03 M (**7**); [H^+]+[Na^+]=0.15 M in samples 6 and 7, 0.15 M NaCl, 25 °C)

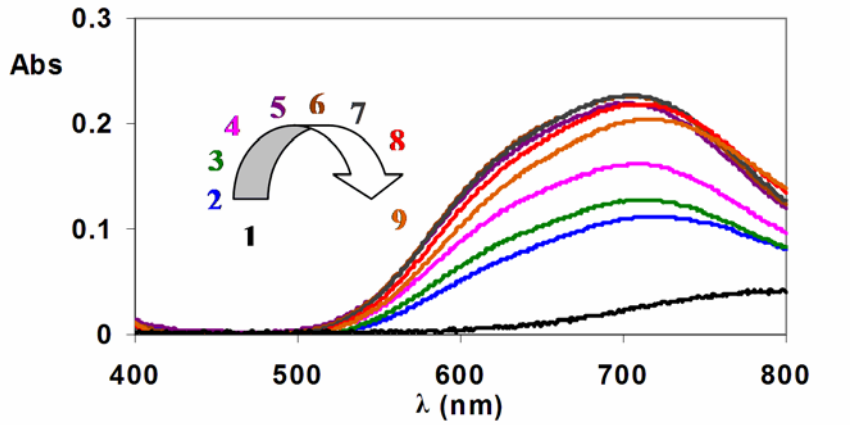

Figure S4: VIS-spectra of Cu^{II}-TRAP systems ([Cu^{II}]=[TRAP]=3.0 mM, [Cu^{II}]=3.0 mM (**1**), [H^+]=1.3 M (**2**), 1.0 M (**3**), 0.7 M (**4**), 0.3 M (**5**), 0.2 (**6**), 0.1 M (**7**), 0.03 M (**8**) and 0.016 M (**9**); [H^+]+[Na^+]=0.15 M in samples 7, 8 and 9, 0.15 M NaCl, 25 °C)

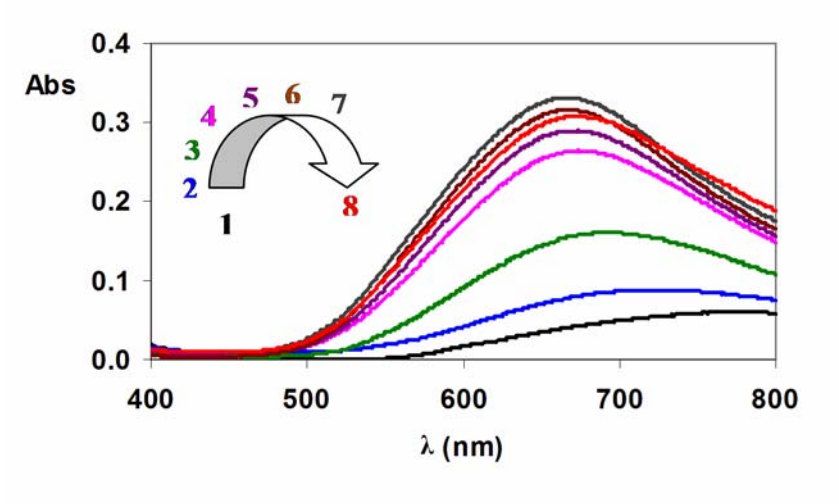

Figure S5: VIS-spectra of Cu^{II}-NOTA systems ([Cu^{II}]=[NOTA]=3.0 mM, [H^+]=1.3 M (**1**), 1.0 M (**2**), 0.7 M (**3**), 0.3 M (**4**), 0.2 (**5**), 0.1 M (**6**), 0.03 M (**7**) and 0.01 M (**8**); [H^+]+[Na^+]=0.15 M in samples 6, 7 and 8, 0.15 M NaCl, 25 °C)

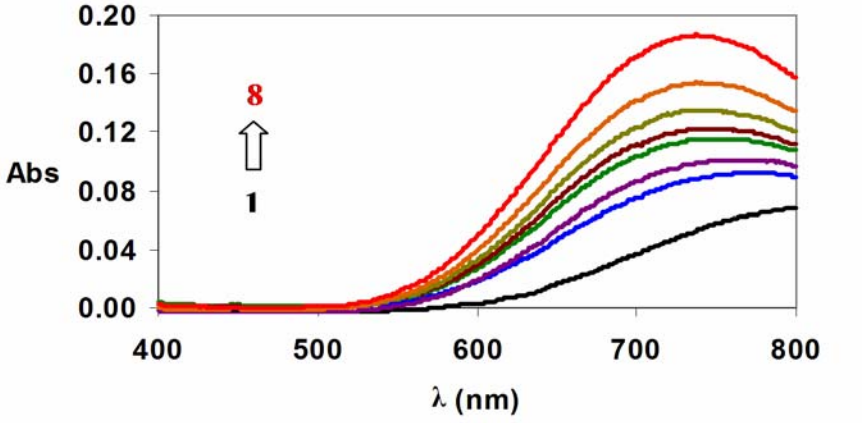

Figure S6: VIS-spectra of Cu^{II}-EDTA systems ([Cu^{II}]=[EDTA]=3.0 mM, [H^+]=1.0 M (**1**), 0.45 M (**2**), 0.32 M (**3**), 0.19 M (**4**), 0.10 (**5**), 0.032 M (**6**), 0.013 M (**7**) and 0.006 M (**8**); [H^+]+[Na^+]=0.15 M in samples 5, 6, 7 and 8, 0.15 M NaCl, 25 °C)

Figures S3–S6 show that absorbances increase λεwith decrease of [H^+], due to formation of [$Cu(H_xL)$] complexes. Since positions of absorption maxima and molar absorptivities of [$Cu(H_xL)$] and Cu^{II} differ considerably (e.g. Cu^{II}: λ_{max} = 800 nm, ε_{800nm}= 13.45 $cm^{-1}\,M^{-1}$; [Cu(HNOTA)]: λ_{max} = 655 nm, ε_{655nm} = 108.6 $cm^{-1}\,M^{-1}$), the stability constants of the CuL complexes have been calculated from the [H^+] and absorbance values obtained at 11 wavelengths between 550 nm and 800 nm, by taking into account the protonation constants of

[CuL] complexes which were determined by pH-potentiometric titration of complexes (Table S1). For calculations, the molar absorptivities of Cu^{II}, [Cu(H_xL)] and [CuL] species have been determined at the same 11 wavelengths in separate experiments. The stability constants of [CuL] complexes are presented in Table S1.

In order to get an insight into solution structures of Cu^{II}-complexes, absorption maxima and molar absorptivities of [CuL] and [Cu(H_xL)] species were analysed in detail. Molar absorptivities of the [Cu(TRAP(CHX)$_3$)], [Cu(TRAP)] and [Cu(NOTA)] complexes are presented in Figures S7–S9.

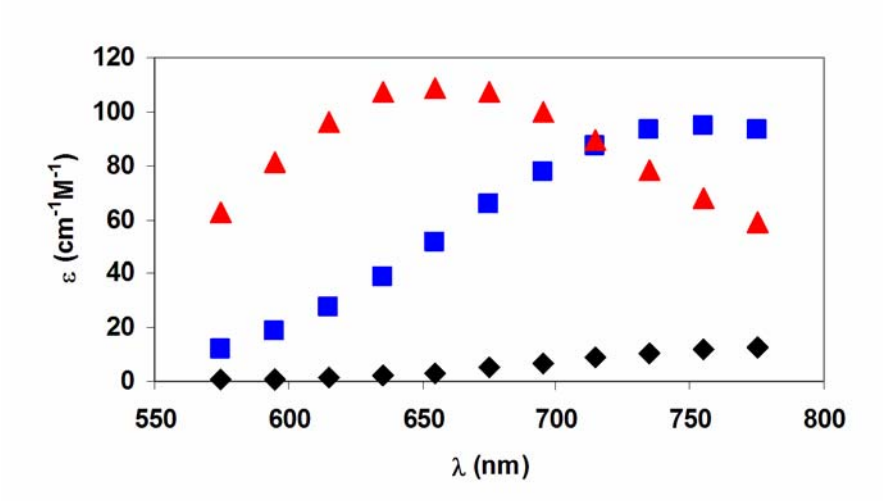

Figure S7: Molar absorptivities of Cu^{II} (♦), [Cu(HNOTA)] (▲) and [Cu(NOTA)] (■) complexes (0.15 M NaCl, 25 °C)

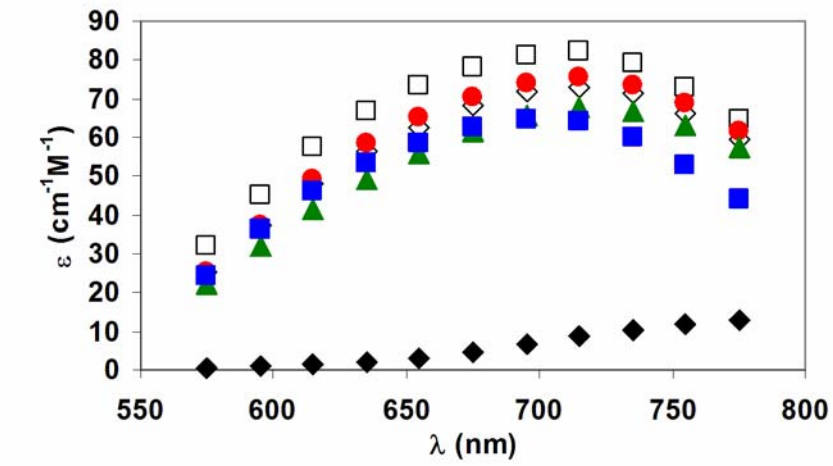

Figure S8: Molar absorptivities of [Cu(TRAP)] complexes (Cu^{II} (♦), [CuL] (□), [Cu(HL)] (◊), [Cu(H_2L)] (●), [Cu(H_3L)] (▲) and [Cu(H_4L)] (■), 0.15 M NaCl, 25 °C)

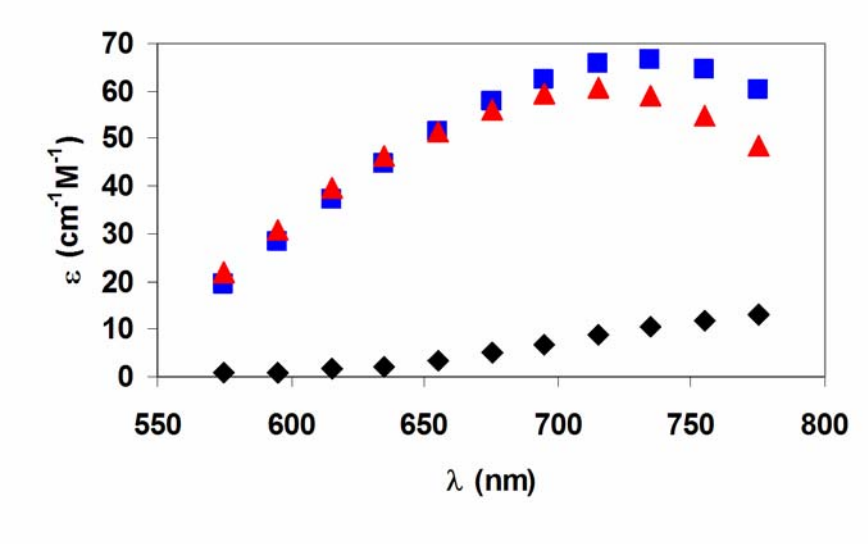

Figure S9: Molar absorptivities of [Cu(TRAP(CHX)$_3$)] complexes (Cu^{II} (♦), [CuL] (■), [Cu(HL)] (▲), 0.15 M NaCl, 25 °C)

Figure S7 shows that the maximum of the absorption band is shifted from 655 to 755 nm upon deprotonation of [Cu(HNOTA)] and formation of [Cu(NOTA)] complex. By assuming that the solution structure of [Cu(HNOTA)] is comparable to that observed in solid state (cf. crystal structure deposited at CCDC, #1025548), the observed red shift of ca. 100 nm can be explained by deprotonation of –COOH and subsequent coordination of the carboxylate group in the empty axial position of Cu^{II}.

The maximum of the absorption bands and ε values of the Cu(TRAP) complexes, presented in Figure S8, are very similar. Deprotonation of [Cu(H_4TRAP)] and formation of [Cu(H_3TRAP)] results in a shift of the absorption maximum from 695 nm to 715 nm. According to the similarity of Cu(NOTA) and Cu(TRAP) complexes, it can be assumed that this red shift of 20 nm is caused by a comparable deprotonation and coordination of the phosphinate oxygen donor atom in the axial position of Cu^{II}. However, the smaller red shift observed upon deprotonation of [Cu(H_4TRAP)] might be attributed to the weaker perturbation effect of the coordinating phosphinate oxygen donor on the d-d transition of Cu^{II} ion, due to the relatively large size of phosphinate group. Deprotonation of [Cu(H_3TRAP)], [Cu(H_2TRAP)], [Cu(HTRAP)] and [Cu(TRAP)] has no influence on the positions of absorption maxima (Figure S8), as they are caused by deprotonation of the non-coordinating carboxylate pendant arms. In the fully deprotonated [Cu(TRAP)], the Cu^{II}-ion should be coordinated by two ring

nitrogen and two phosphinate oxygen atoms in equatorial positions, and by a ring nitrogen and a phosphinate oxygen atom in axial positions.

Spectrophotometric studies of the [Cu(TRAP(CHX)$_3$)] complex indicates formation of [Cu(HL)] and [CuL] species, characterized by different absorption spectra (Figure S9). The position of the absorption maximum is shifted from 715 nm to 735 nm upon deprotonation of [Cu(HTRAP(CHX)$_3$)] and formation of [Cu(TRAP(CHX)$_3$)]. Similar to the [Cu(H$_4$TRAP)] complex, this red shift of ca. 20 nm can be explained by deprotonation and subsequent coordination of the phosphinate oxygen donor. According to the similar absorption spectra and ε values, it can be assumed that the solution structures of the deprotonated [Cu(TRAP(CHX)$_3$)] and [Cu(TRAP)] complexes are highly similar.

Stability constants of Ca^{II}, Zn^{II} and Cu^{II} complexes formed with TRAP(CHX)$_3$ and TRAP (Table S1) are generally about 5–6 orders of magnitude lower than those of the corresponding complexes of NOTA. The lower stability of the TRAP(CHX)$_3$ and TRAP complexes can be explained by lower basicity of the ring nitrogens and phosphinate oxygen atoms. The complexes formed with TRAP can be easily protonated, due to the presence of non-coordinating carboxylate groups of the pendant arms. However, these carboxylate groups can also engage in coordination of a second metal ion, resulting in formation of homo- and hetero-dinuclear complexes. Stability constants ($\log K_{M*(ML)}$) of such complexes are generally quite low (Table S2), which indicates that just one or two carboxylate groups are coordinated to the second metal ion. Moreover, pH-potentiometric titrations indicate a facile protonation of the dinuclear species, which confirms that coordination of the second metal ion is effected by one or two carboxylate groups of the pendant arms.

For TRAP(CHX)$_3$, formation of the protonated complex was observed in the case of [Cu(TRAP(CHX)$_3$)]. Since further deprotonation could not be observed by either pH-potentiometry or UV-spectrophotometry, deprotonation and coordination of the amide groups to Cu^{II}-ion can be ruled out.

Table S1: Stability and protonation constants of Ca^{II}-, Zn^{II}- and Cu^{II}-complexes formed with $TRAP(CHX)_3$, TRAP and NOTA ligands (25°C)

	$TRAP(CHX)_3$	**TRAP**		**NOTA**	
I	0.15 M NaCl	0.15 M NaCl	0.1 M Me_4NCl[3]	0.15 M NaCl	0.1 M Me_4NCl[8]
CaL	**4.90 (4)**	**7.35 (2)**	**6.04**	**9.31 (3)**	**10.32**
CaHL	–	7.41 (3)	7.94	5.21 (9)	–
CaH_2L	–	4.90 (5)	4.98	–	–
Ca_2L	–	1.0 (8)	2.80	–	–
ZnL	**15.15 (6)** (pH-pot) **15.75 (5)** (NMR)	**16.07 (3)** (pH-pot.) **16.39 (6)** (NMR)	**16.88**	**21.56 (5)** (NMR)	**21.58**
ZnHL	–	6.16 (3)	5.17	1.29 (4) (NMR)	–
ZnH_2L	–	4.62 (3)	4.68	–	–
ZnH_3L	–	3.88 (3)	3.96	–	–
ZnH_4L	–	–0.4 (1) (NMR)	–	–	–
Zn_2L	–	3.14 (4)	2.43	–	–
Zn_2LH	–	4.87 (9)	4.71	–	–
CuL	**17.63 (4)** (VIS)	**19.09 (3)** (VIS)	**16.85**	**22.44 (3)** (VIS)	**21.99**
CuHL	1.97 (1)	5.18 (2)	5.14	2.64 (2)	2.54
CuH_2L	–	4.47 (2)	4.66	–	
CuH_3L	–	4.01 (2)	3.95	–	
CuH_4L	–	1.58 (2)	1.33	–	
Cu_2L	–	3.14 (6)	3.32	–	
Cu_2LH	–	4.71 (5)	4.79	–	

Table S2: Stability and protonation constants of the hetero-dinuclear Ca^{II}-, Zn^{II}- and Cu^{II}-TRAP complexes (0.15 M NaCl, 25°C):

	Cu[Zn(L)]	**Ca[Zn(L)]**	**Zn[Cu(L)]**	**Ca[Cu(L)]**
$\log K_{M*(ML)}$	2.11 (6)	1.76 (8)	2.30 (6)	1.13 (9)
$\log K_{M*(MHL)}$	5.42 (6)	5.83 (9)	4.80 (6)	5.96 (9)

3. Kinetic studies of the ligand exchange reaction of [Cu(TRAP(CHX)$_3$)] and Cu(TRAP) with EDTA and NOTA

The ligand exchange reactions of Cu(TRAP(CHX)$_3$) and Cu(TRAP) with EDTA and NOTA were studied by UV-spectrophotometry, see Eq. (10),

$$Cu(H_xL) + H_yA \rightleftharpoons Cu(H_zA) + H_sL \qquad (10)$$

wherein for TRAP(CHX)$_3$: x = 0, 1; s = 2, 3; TRAP: x = 3, 4; s = 4, 5, 6; NOTA: y = 3, 4; z = 0, 1; EDTA: y = 3, 4, z = 0, 1, 2).

The absorption spectra of the Cu(TRAP(CHX)$_3$) + EDTA, Cu(TRAP) + EDTA, Cu(TRAP(CHX)$_3$) + NOTA, and Cu(TRAP) + NOTA reactions is shown in Figures S10–S13. The obtained pseudo-first-order rate constants (k_d) are shown in Figure 1 (main text).

Figure 1 shows that the reaction rates are independent from the concentration of the competing ligands NOTA and EDTA. Hence, it can be assumed that ligand exchange reactions of Cu(TRAP(CHX)$_3$) and Cu(TRAP) take place by spontaneous dissociation of the complex, followed by a fast reaction between the released Cu^{II} ion and free NOTA / EDTA, as exemplified by Figure S14.

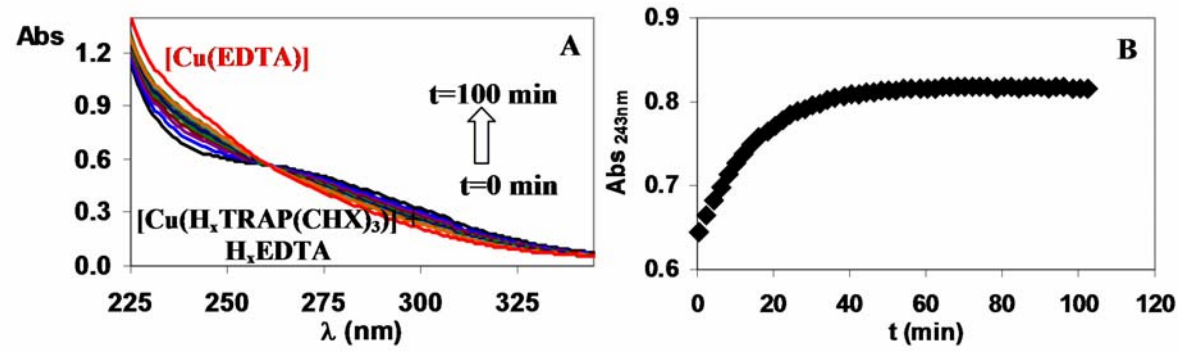

Figure S10: Absorption spectra (A) and kinetic curve (B) of the transmetallation reaction between [Cu(H_xTRAP(CHX)$_3$)] and H_xEDTA ([Cu(H_xTRAP(CHX)$_3$)]=0.2 mM (x=0,1), [EDTA]=4.0 mM, [DCA]=0.01 M, pH=2.04, 0.15 M NaCl, 25°C)

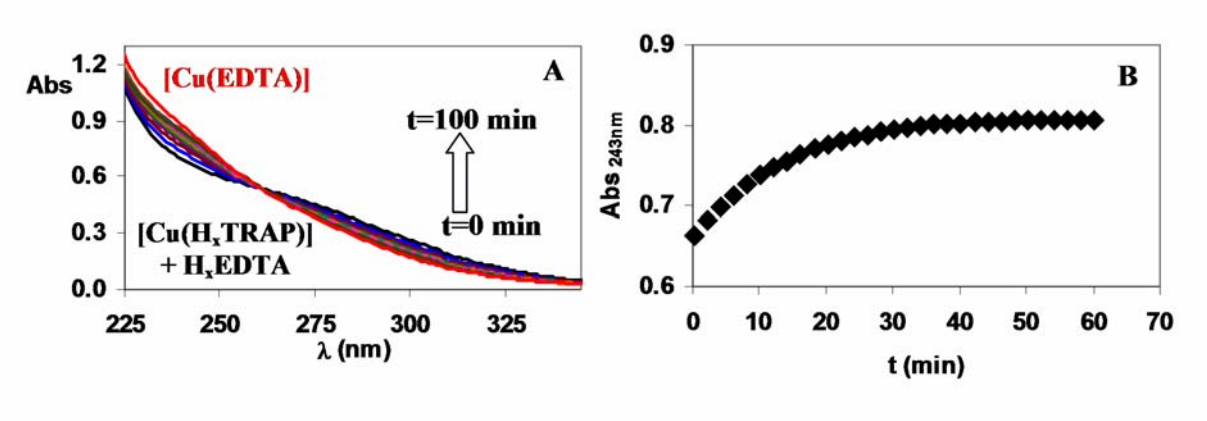

Figure S11: Absorption spectra (A) and kinetic curve (B) of the transmetallation reaction between [Cu(H_xTRAP)] and H_xEDTA ([Cu(H_xTRAP)]=0.2 mM, [EDTA]=4.0 mM, [DCA]=0.01 M, pH=2.07, 0.15 M NaCl, 25°C)

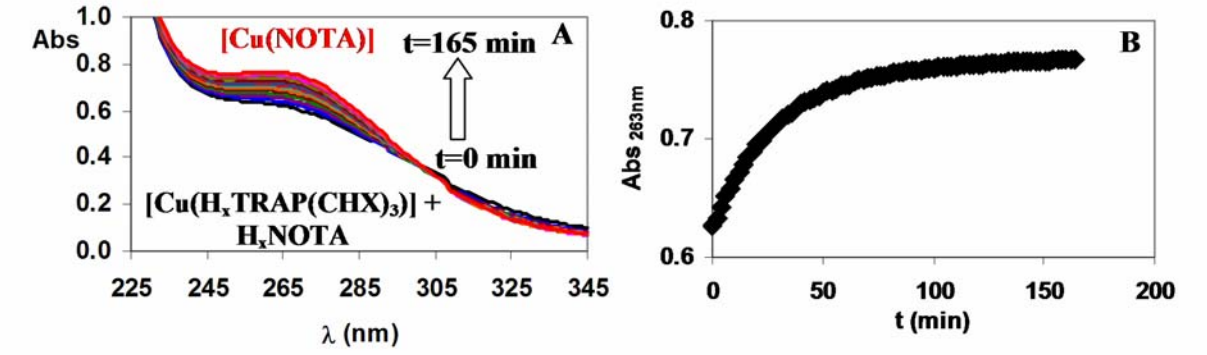

Figure S12: Absorption spectra (A) and kinetic curve (B) of the transmetallation reaction between [Cu(H_xTRAP(CHX)$_3$)] and H_xNOTA ([Cu(H_xTRAP(CHX)$_3$)]=0.2 mM (x=0,1), [NOTA]=2.0 mM, [DCA]=0.01 M, pH=1.97, 0.15 M NaCl, 25°C)

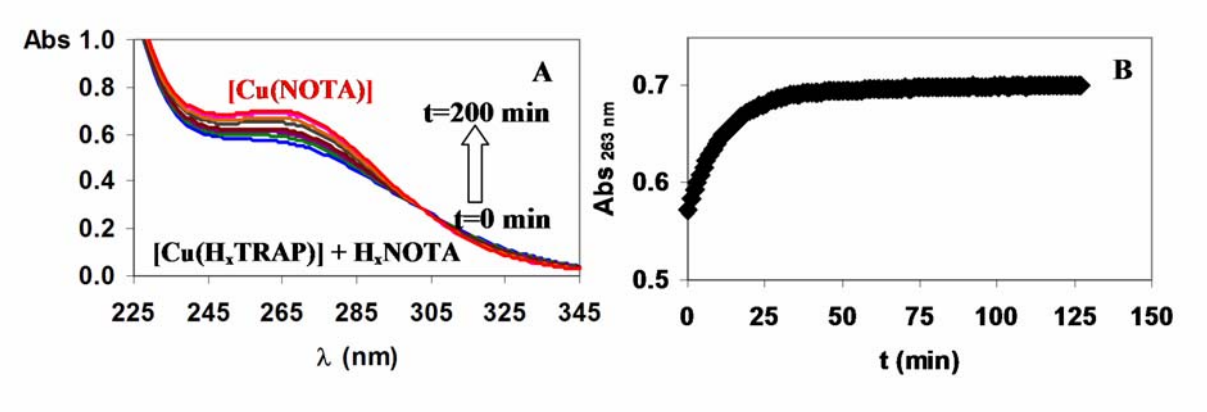

Figure S13: Absorption spectra (A) and kinetic curve (B) of the transmetallation reaction between [Cu(H_xTRAP)] and H_xNOTA ([Cu(H_xTRAP)]=0.2 mM, [NOTA]=2.0 mM, [DCA]=0.01 M, pH=1.82, 0.15 M NaCl, 25°C)

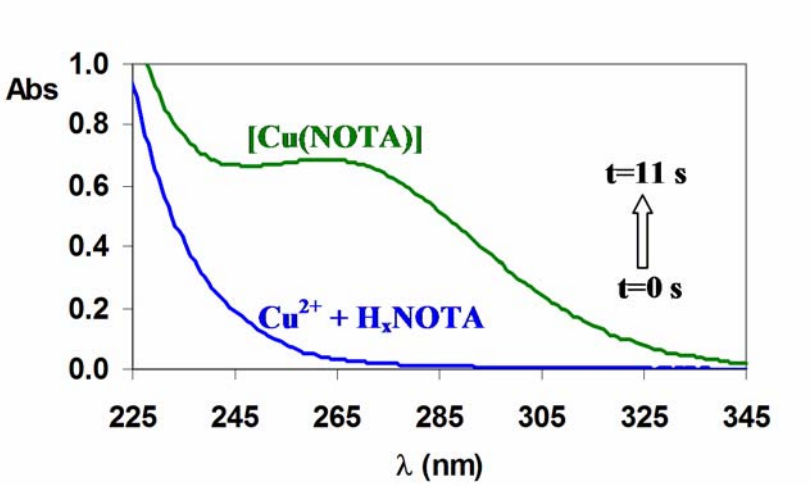

Figure S14: Absorption spectra of the Cu^{II}-NOTA reacting system before and 11 s after mixing ([Cu^{II}]=0.2 mM, [H_xNOTA]=2.0 mM, [DCA]=0.01 M, pH=1.78, 0.15 M NaCl, 25°C)

In presence of excess of NOTA or EDTA, the ligand exchange reactions of Cu(TRAP(CHX)$_3$) and Cu(TRAP) can be treated as pseudo-first-order processes, and reaction rates can be described by Eq. (11), wherein k_d is a pseudo-first-order rate constant, and $[CuL]_t$ and $[CuL]_{tot}$ are the concentrations of the CuL containing species at time t and at the start of the reaction, respectively.

$$-\frac{d[CuL]_t}{dt} = k_d[CuL]_{tot} \qquad (11)$$

Figure 1 shows that the dissociation rate of Cu(TRAP) is proportional to the H^+ concentration. With regard to the protonation constants of Cu(TRAP) ($\log K_{CuHL}$=5.18, $\log K_{CuH2L}$=4.47, $\log K_{CuH3L}$=4.01 and $\log K_{CuH4L}$=1.58) and the pH range of the kinetic studies (pH = 1.5–4.0), ligand exchange reactions between diprotonated [$Cu(H_2TRAP)$], triprotonated [$Cu(H_3TRAP)$] and tetraprotonated [$Cu(H_4TRAP)$], and EDTA or NOTA have to be considered. The increase of k_d values with H^+ concentration can be interpreted in terms of *i*) spontaneous dissociation of diprotonated [$Cu(H_2TRAP)$] (Eq. (12)), *ii*) formation and spontaneous dissociatiation of triprotonated [$Cu(H_3TRAP)$] (Eqs. (13) and (14)), *iii*) formation and spontaneous dissociatiation of tetraprotonated [$Cu(H_4TRAP)$] (Eqs. (15) and (16)).

$$CuH_2L \xrightarrow{k_0} Cu^{2+} + H_xL \quad \textit{Spontaneous dissociation of [Cu(H}_2\textit{L)]} \quad (12)$$

$$CuH_2L + H^+ \overset{K^H_{CuH_2L}}{\rightleftharpoons} CuH_3L \quad \textit{Protonation of [Cu(H}_2\textit{L)]} \quad (13)$$

$$K^H_{CuH_2L} = \frac{[CuH_3L]}{[CuH_2L][H^+]}$$

$$CuH_3L \xrightarrow{k_{CuH_3L}} Cu^{2+} + H_xL \quad \textit{Spontaneous dissociation of [Cu(H}_3\textit{L)]} \quad (14)$$

$$CuH_3L + H^+ \overset{K^H_{CuH_3L}}{\rightleftharpoons} CuH_4L \quad \textit{Protonation of [Cu(H}_3\textit{L)]} \quad (15)$$

$$K^H_{CuH_3L} = \frac{[CuH_4L]}{[CuH_3L][H^+]}$$

$$CuH_4L \xrightarrow{k_{CuH_4L}} Cu^{2+} + H_xL \quad \textit{Spontaneous dissociation of [Cu(H}_4\textit{L)]} \quad (16)$$

The rate constants k_0, k_{CuH_3L} and k_{CuH_4L} characterize the spontaneous dissociation of [$Cu(H_2TRAP)$], [$Cu(H_3TRAP)$] and [$Cu(H_4TRAP)$] complexes, respectively. By considering all possible reaction pathways, the overall rate of the dissociation reaction of Cu(TRAP) according to Eq. (11) can be described by Eq. (17).

$$-\frac{d[CuL]_t}{dt} = k_0[CuH_2L] + k_{CuH_3L}[CuH_3L] + k_{CuH_4L}[CuH_4L] \qquad (17)$$

Wht respect to the total concentration of the complex ($[CuL]_{tot} = [Cu(H_2L)] + [Cu(H_3L)] + [Cu(H_4L)]$) and the protonation constants ($K^{H}_{CuH_2L}$ and $K^{H}_{CuH_3L}$) of $Cu(H_2L)$ and $Cu(H_3L)$ (Eqs. (13) and (15)), the pseudo-first-order rate constant (k_d) can be expressed as follows:

$$k_d = \frac{k_0 + k_1[H^+] + k_2[H^+]^2}{1 + K^{H}_{CuH_2L}[H^+] + K^{H}_{CuH_2L}K^{H}_{CuH_3L}[H^+]^2} \qquad (18)$$

wherein k_0, k_1 ($= k_{CuH_3L} \times K^{H}_{CuH_2L}$) and k_2 ($= k_{CuH_4L} \times K^{H}_{CuH_2L} \times K^{H}_{CuH_3L}$) are the rate constants characterizing the spontaneous dissociation of $[Cu(H_2TRAP)]$, $[Cu(H_3TRAP)]$ and $[Cu(H_4TRAP)]$, respectively. Values for k_0, k_1, k_2 and $K^{H}_{CuH_3L}$ were calculated by fitting the data points in Figure 1 to Eq. (18).

With regard to the protonation constant of $[Cu(TRAP(CHX)_3)]$ ($\log K_{CuHL}=1.97$) and the pH range of the kinetic studies (pH=1.5–4.0), ligand exchange reactions between deprotonated $[Cu(TRAP(CHX)_3)]$ and monoprotonated $[Cu(HTRAP(CHX)_3)]$ and the respective competitor have to be considered. The increase in k_d values with increasing H^+ concentration can be interpreted by spontaneous dissociation of deprotonated $[Cu(TRAP(CHX)_3)]$ (Eq. (19)) and formation and spontaneous dissociatiation of monoprotonated $[Cu(HTRAP(CHX)_3)]$ (Eqs. (20) and (21)).

$$CuL \xrightarrow{k_0} Cu^{2+} + H_xL \qquad \textit{Spontaneous dissociation of [CuL] (19)}$$

$$CuL + H^+ \overset{K^{H}_{CuL}}{\rightleftharpoons} CuH_3L \qquad \textit{Protonation of [CuL] (20)}$$

$$K^{H}_{CuL} = \frac{[CuHL]}{[CuL][H^+]}$$

$$CuHL \xrightarrow{k_{CuHL}} Cu^{2+} + H_xL \qquad \textit{Spontaneous dissociation of [Cu(HL)] (21)}$$

The rate constants k_0 and k_{CuHL} characterize the spontaneous dissociation of $[Cu(TRAP(CHX)_3)]$ and $[Cu(HTRAP(CHX)_3)]$ complexes, respectively. By considering all possible reaction pathways, the overall rate of the dissociation reaction of $Cu(TRAP(CHX)_3)$ according to Eq. (11) can be expressed by Eq. (22).

$$-\frac{d[CuL]_t}{dt} = k_0[CuL] + k_{CuHL}[CuHL] \qquad (22)$$

With respect to the total concentration of the complex ($[CuL]_{tot}=[CuL]+[CuHL]$) and the protonation constant (K^{H}_{CuL}) of [Cu(TRAP(CHX)$_3$)] (Eq. (20)), the pseudo-first-order rate constant (k_d) can be expressed as follows:

$$k_d = \frac{k_0 + k_1[H^+]}{1 + K^{H}_{CuL}[H^+]} \qquad (23)$$

wherein k_0 and k_1 ($= k_{CuHL} \times K^{H}_{CuL}$) are the rate constants characterizing the spontaneous dissociation of [Cu(TRAP(CHX)$_3$)] and [Cu(HTRAP(CHX)$_3$)], respectively. The k_0, k_1 and K^{H}_{CuL} values have been calculated by fitting the data points in Figure 1 to Eq. (23). Rate (k) and equilibrium (K) constants characterizing the ligand exchange reaction of Cu(TRAP(CHX)$_3$) and Cu(TRAP) with NOTA and EDTA are summarized in Table S3.

Considering the pH range investigated (1.7–4.0) and the different speciation of the Cu(TRAP(CHX)$_3$) and Cu(TRAP) complexes, ligand exchange reactions occur between EDTA/NOTA and deprotonated [Cu(TRAP(CHX)$_3$)], monoprotonated [Cu(HTRAP(CHX)$_3$)], diprotonated [Cu(H_2TRAP)], triprotonated [Cu(H_3TRAP)] and tetraprotonated [Cu(H_4TRAP)] complexes. Generally, the rate determining step is the dissociation of Cu(TRAP(CHX)$_3$) and Cu(TRAP) complexes, followed by fast reactions of free Cu^{II} with EDTA or NOTA. For Cu(TRAP(CHX)$_3$), the reaction proceeds by spontaneous dissociation of the deprotonated (k_0) and monoprotonated (k_1) complexes. For Cu(TRAP), k_0, k_1, and k_2 characterize the spontaneous dissociation of the di-, tri-, and tetraprotonated complexes, respectively.

Table S3: The rate (k) and equilibrium (K) constants characterizing the ligand exchange reaction of [Cu(TRAP(CHX)$_3$)] and [Cu(TRAP)] with NOTA and EDTA (0.15 M NaCl, 25°C)

	[Cu(TRAP(CHX)$_3$)]	**[Cu(TRAP)]**
k_0 (s^{-1})	$(6 \pm 4)\times10^{-7}$	$(5 \pm 3)\times10^{-6}$
k_1 ($M^{-1}s^{-1}$)	$(7.0 \pm 0.2)\times10^{-2}$	0.69 ± 0.03
k_2 ($M^{-1}s^{-1}$)	–	790 ± 58
K^{H}_{CuL} (M^{-1})	30 ± 4	–
$K^{H}_{CuH_2L}$ (M^{-1})	–	10233 (pH-pot.)
$K^{H}_{CuH_3L}$ (M^{-1})	–	37 ± 8
k_d (s^{-1}) at pH=4.0	7.0×10^{-6}	3.5×10^{-5}
$\tau_{1/2}$ (h) at pH=4.0	23.9	5.1

For the direct comparison of the kinetic inertness, the dissociation rates (k_d) and half-lives ($t_{1/2}=\ln2/k_d$) of [Cu(TRAP(CHX)$_3$)] and [Cu(TRAP)] were calculated for the pH=4.0 by using the rate and protonation constants reported in Table S3 (k_d values of [Cu(TRAP)] and [Cu(TRAP(CHX)$_3$)] were calculated by the use of Eqs. (18) and (22), respectively. The dissociation half-lives ($\tau_{1/2}$) of [Cu(TRAP(CHX)$_3$)] and [Cu(TRAP)] are 23.9 and 5.1 hours indicating the higher kinetic inertness of the [Cu(TRAP(CHX)$_3$)] at pH=4.0.

The rate of the exchange reactions of [Cu(TRAP(CHX)$_3$)] and [Cu(TRAP)] with NOTA were also determined at 288, 310 and 323 K in order to calculate the activation parameters governing the dissociation reactions of [Cu(TRAP(CHX)$_3$)] and [Cu(TRAP)]. The rate (k) and equilibrium (K) constants characterizing the ligand exchange reaction of [Cu(TRAP(CHX)$_3$)] and [Cu(TRAP)] with NOTA at 288, 298, 310 and 323 K are summarized in Table S4.

Table S4: The rate (k) and equilibrium (K) constants characterizing the ligand exchange reaction of Cu(TRAP(CHX)$_3$) and Cu(TRAP) with NOTA at 288, 298, 310 and 323 K

	[Cu(TRAP(CHX)$_3$)]			[Cu(TRAP)]				
T (K)	k_0 (s^{-1})	k_1 ($M^{-1}s^{-1}$)	K^{H}_{CuL} (M^{-1})	k_0 (s^{-1})	k_1 ($M^{-1}s^{-1}$)	k_2 ($M^{-1}s^{-1}$)	$K^{H}_{CuH_2L}$ (M^{-1})	$K^{H}_{CuH_3L}$ (M^{-1})
288	–	(2.1±0.2) ×10^{-2}	38 ± 8	(3 ± 9) ×10^{-7}	(1.7±0.2) ×10^{-1}	(3.0±0.1) ×10^{2}	10233 (fix)	41 ± 6
298	(6 ± 2) ×10^{-7}	(7.0±0.2) ×10^{-2}	30 ± 4	(5 ± 3) ×10^{-6}	(6.9±0.3) ×10^{-1}	(7.9±0.6) ×10^{2}	10233 (fix)	37 ± 8
310	(2 ± 1) ×10^{-6}	(2.6±0.1) ×10^{-1}	24 ± 7	(3 ± 6) ×10^{-8}	2.7±0.2	(2.7±0.2) ×10^{3}	10233 (fix)	36 ± 10
323	(3 ± 1) ×10^{-5}	(6.6±0.2) ×10^{-1}	30 ± 5	(6 ± 8) ×10^{-7}	5.8±0.5	(6.7±0.4) ×10^{3}	10233 (fix)	30 ± 7

The k_0 rate constants of [Cu(TRAP)] are very low and the error in them is very high, indicating the unimportance of the spontaneous dissociation of the [Cu(H_2TRAP)]. However, the k_0 and k_1 rate constant characterizing the spontaneous dissociation of [Cu(TRAP(CHX)$_3$)] and [Cu(HTRAP(CHX)$_3$)], k_1 and k_2 rate constants related to the spontaneous dissociation of [Cu(H_3TRAP)] and [Cu(H_4TRAP)] complexes increase with the increase of temperature which can be explained by the faster intramolecular rearrangement of the Cu^{II}-complexes results in the faster dissociation reaction at higher temperature. Interestingly, the protonation constant of [Cu(TRAP(CHX)$_3$)] (K^{H}_{CuL}) and [Cu(TRAP)] ($K^{H}_{CuH_3L}$) complexes are not effected by the temperature. Similar phenomena have been observed for Zn^{II}- and Cu^{II}-complexes formed with DTPA-derivatives.[9] Because of the $K^{H}_{CuH_3L}$ protonation constant of [Cu(TRAP)] was not influenced by the temperature, the $K^{H}_{CuH_2L}$ value of [Cu(TRAP)] was fixed to 10233 M^{-1} (determined by pH-potentiometric studies at 298K) in order to obtain the best fitting of the experimental data.

By taking into account the k_0, $k_1 = k_{CuHL} \times K^{H}_{CuL}$ and K^{H}_{CuL} values for [Cu(TRAP(CHX)$_3$)] and $k_1 = k_{CuH_3L} \times K^{H}_{CuH_2L}$, $k_2 = k_{CuH_4L} \times K^{H}_{CuH_2L} \times K^{H}_{CuH_3L}$, $K^{H}_{CuH_2L}$ and

$K^{H}_{CuH_3L}$ values for [Cu(TRAP)] obtained at 288, 298, 310 and 323 K, k_{CuL}, k_{CuHL}, k_{CuH_3L} and k_{CuH_4L} rate constants characterize the spontaneous dissociation of [Cu(TRAP(CHX)$_3$)], [Cu(HTRAP(CHX)$_3$)], [Cu(H$_3$TRAP)] and [Cu(H$_4$TRAP)] complexes were calculated, respectively. The activation parameters (Table 3) characterizing the spontaneous dissociation of [Cu(TRAP(CHX)$_3$)], [Cu(HTRAP(CHX)$_3$)], [Cu(H$_3$TRAP)] and [Cu(H$_4$TRAP)] complexes were determined by the use of the the *Eyring* equation. The *Eyring* plots for the calculation of the activation parameters for the spontaneous dissociation of [Cu(TRAP(CHX)$_3$)], [Cu(HTRAP(CHX)$_3$)], [Cu(H$_3$TRAP)] and [Cu(H$_4$TRAP)] complexes are shown in Figure S15.

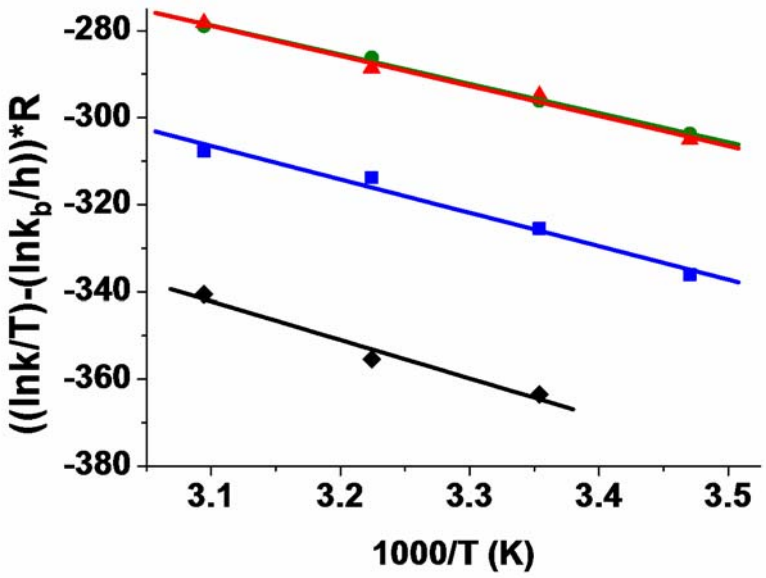

Figure S15: Eyring plots for determining the activation parameters of the spontaneous dissociation reactions of **[Cu(H$_3$TRAP)]** (■), **[Cu(H$_4$TRAP)]** (●), **[Cu(TRAP(CHX)$_3$)]** (♦) and **[Cu(HTRAP(CHX)$_3$)]** (▲)

Our kinetic studies provides very similar activation enthalpy ($\Delta H^{\ddagger}$) activation entropy ($\Delta S^{\ddagger}$), activation free energy ($\Delta G^{\ddagger}_{298}$) and rate constant ($k^{298}$) values for the spontaneous dissociation of [Cu(H$_4$TRAP)] and [Cu(HTRAP(CHX)$_3$)] complexes. However, the spontaneous dissociation of [Cu(H$_3$TRAP)] and [Cu(TRAP(CHX)$_3$)] are characterized by higher activation enthalpy ($\Delta H^{\ddagger}$), activation free energy ($\Delta G^{\ddagger}_{298}$) and by lover rate constant (k^{298}) values. By taking into account these observation, it can be assumed that the reaction pathway and rate determining step of the spontaneous dissociation of [Cu(H$_4$TRAP)] and [Cu(HTRAP(CHX)$_3$)]

are very similar and differs from that of [Cu(H_3TRAP)] and [Cu(TRAP$(CHX)_3$)]. The spontaneous dissociation of the [Cu(H_4TRAP)] and [Cu(HTRAP$(CHX)_3$)] probably takes place by the proton transfer from the protonated phosphinate group to the ring nitrogen atoms results in the dissociation of the Cu^{II}-complexes. Because of the structure of the [Cu(H_4TRAP)] and [Cu(HTRAP$(CHX)_3$)] are similar (one of the phosphinate oxygen atom is protonated), it can be assumed that the proton transfer from the protonated phosphinate group to the ring nitrogen atoms is characterized with very similar activation barrier. The spontaneous dissociation of [Cu(H_3TRAP)] probably takes place by the proton transfer from the protonated carboxylate group to the phosphinate group and finally to the ring nitrogen atoms results in the dissociation of the Cu^{II}-complex. However, the protonation of the phosphinate group can take place by the decoordination of the phosphinate oxygen donor atom in [Cu(H_3TRAP)]. The higher activation enthalpy ($\Delta H^{\ddagger}$), activation free energy ($\Delta G^{\ddagger}_{298}$) and lover rate constant (k^{298}) value of the spontaneous dissociation of [Cu(H_3TRAP)] can be interpreted by the decoordination of the phosphinate oxygen donor atom which might be responsible for the higher energy level of the transition state. The spontaneous dissociation of [Cu(TRAP$(CHX)_3$)] complex is characterized by higher activation enthalpy ($\Delta H^{\ddagger}$), activation free energy ($\Delta G^{\ddagger}_{298}$) and by lover rate constant (k^{298}) values The spontaneous dissociation [Cu(TRAP$(CHX)_3$)] complex probably takes place by the proton transfer from the amide group to the coordinated phosphinate group or by the water assisted protonation of the coordinated phosphinate group which is followed by the proton transfer to the ring nitrogen atoms results in the dissociation of the Cu^{II}-complex. Both reaction pathways are characterized by higher activation barrier as it was found for the [Cu(TRAP$(CHX)_3$)], [Cu(H_3TRAP)] and [Cu(H_4TRAP)] complexes.

The spontaneous dissociation of [Cu(TRAP$(CHX)_3$)], [Cu(HTRAP$(CHX)_3$)], [Cu(H_3TRAP)] and [Cu(H_4TRAP] complexes are characterized by negative activation entropy values ($\Delta S^{\ddagger}$), which is probably related to the reorganization of the hydration shell around the Cu^{II}-ion in the transition state.

4. References

1 J. Notni, J. Šimeček, P. Hermann and H. J. Wester, *Chem. Eur. J.,* 2011, **17**, 14718–14722.

2 M. Weineisen, J. Simecek, M. Schottelius, M. Schwaiger and H. J. Wester, *EJNMMI Res.*, 2014, **4**, 36.

3 J. Notni, P. Hermann, J. Havlíčková, J. Kotek, V. Kubíček, J. Plutnar, N. Loktionova, P. J. Riss, F. Rösch and I. Lukeš, *Chem. Eur. J.,* 2010, **16**, 7174–7185.

4 J. Notni, J. Šimeček, P. Hermann and H. J. Wester, *Chem. Eur. J.,* 2011, **17**, 14718–14722.

5 J. Notni, K. Pohle and H. J. Wester, *Nucl. Med. Biol.,* 2012, **39**, 777–784.

6 H. M. Irving, M. G. Miles and L. D. Pettit, *Analytica Chimica Acta*, 1967, **38**, 475–488.

7 L. Zekany and I. Nagypal, ed. D. J. Leget, Plenum Press, New York, 1985, pp. 291–353.

8 J. Šimeček, M. Schulz, J. Notni, J. Plutnar, V. Kubíček, J. Havlíčková and P. Hermann, *Inorg. Chem.,* 2012, **51**, 577–590.

9 Z. Baranyai, E. Brücher, F. Uggeri, A. Maiocchi, I. Tóth, M. Andrási, A. Gáspár, L. Zékány and S. Aime, *Chem. Eur. J.*, 2014, in press.

Appendix:

Distribution diagrams

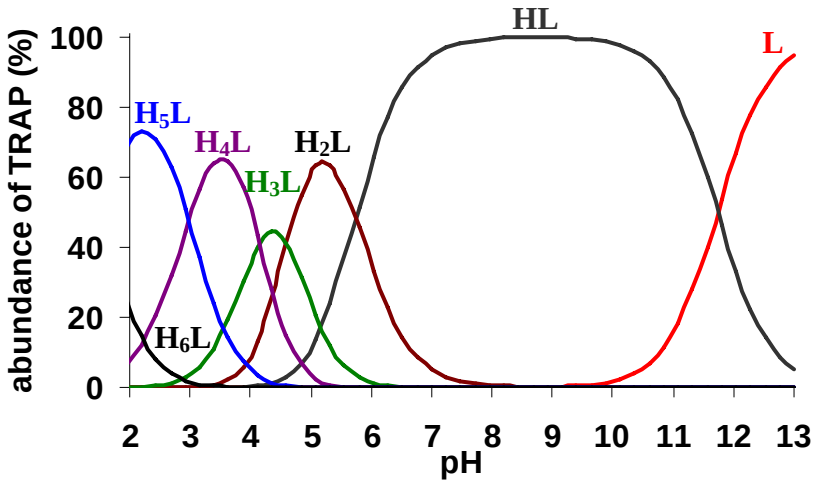

Figure A1. Species distribution of TRAP ([TRAP]=2.0 mM, 0.15 M NaCl, 298 K)

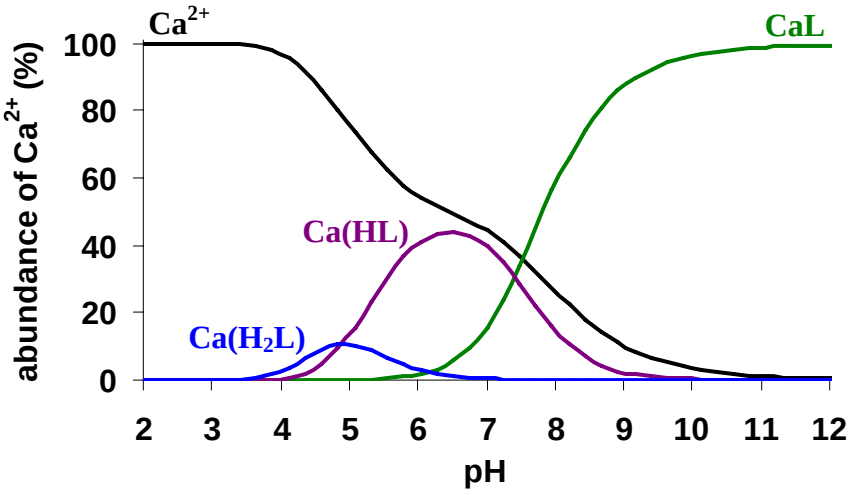

Figure A2. Species distribution of Ca^{2+} - TRAP system ([Ca^{2+}]=[TRAP]=2.0 mM, 0.15 M NaCl, 298 K)

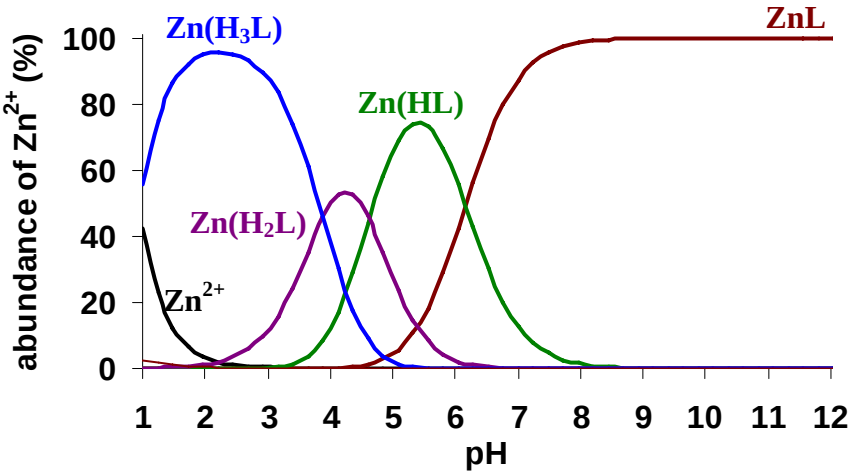

Figure A3. Species distribution of Zn^{2+} - TRAP system ([Zn^{2+}]=[TRAP]=2.0 mM, 0.15 M NaCl, 298 K)

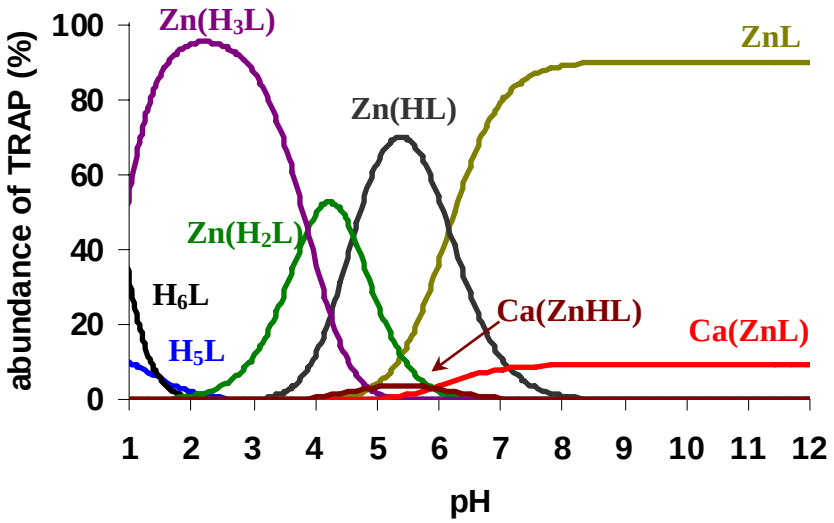

Figure A4. Species distribution of Ca^{2+} - Zn^{2+} - TRAP system ([Ca^{2+}]=[Zn^{2+}]=[TRAP]=2.0 mM, 0.15 M NaCl, 298 K)

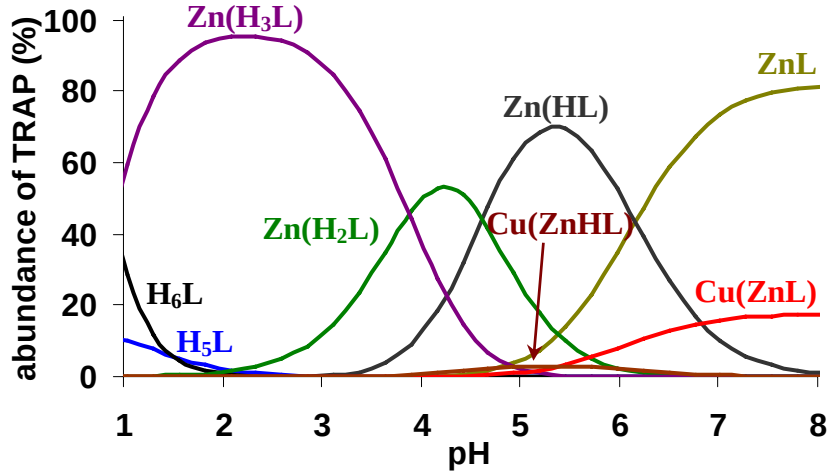

Figure A5. Species distribution of Cu^{2+} -Zn^{2+} - TRAP system ([Cu^{2+}]=[Zn^{2+}]=[TRAP]=2.0 mM, 0.15 M NaCl, 298 K)

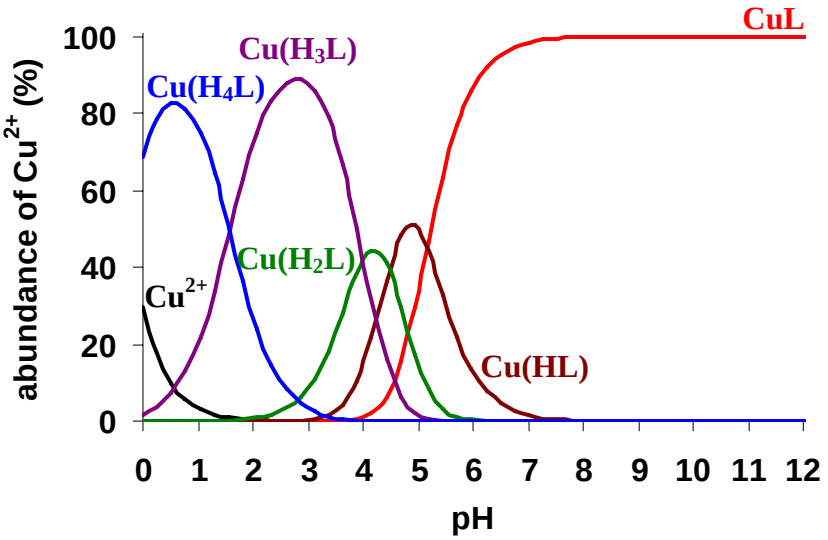

Figure A6. Species distribution of Cu^{2+} - TRAP system ([Cu^{2+}]=[TRAP]=2.0 mM, 0.15 M NaCl, 298 K)

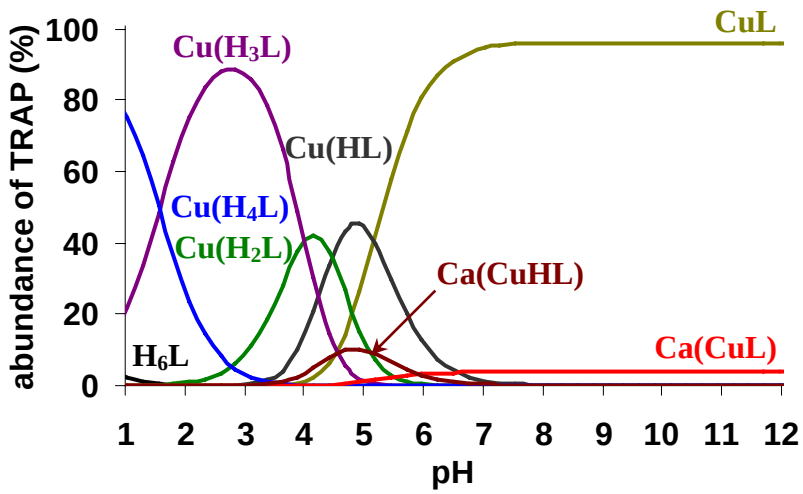

Figure A7. Species distribution of Ca^{2+} - Cu^{2+} - TRAP system ([Ca^{2+}]=[Cu^{2+}]=[TRAP]=2.0 mM, 0.15 M NaCl, 298 K)

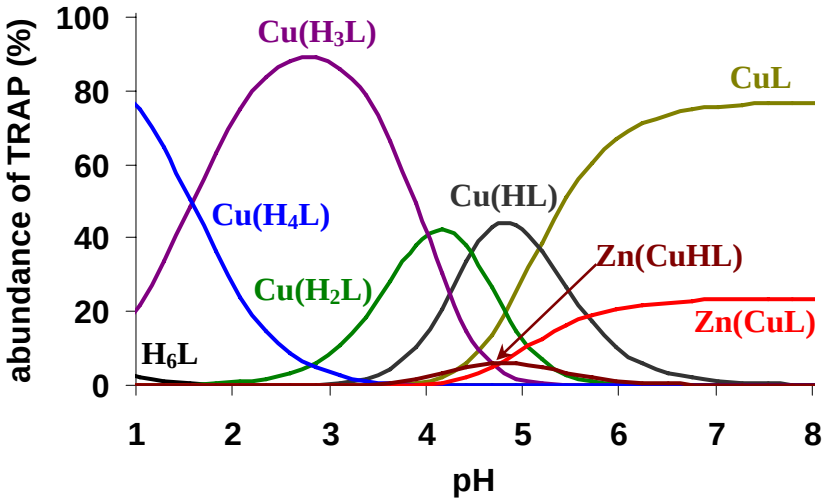

Figure A8. Species distribution of Zn^{2+} - Cu^{2+} - TRAP system ([Zn^{2+}]=[Cu^{2+}]=[TRAP]=2.0 mM, 0.15 M NaCl, 298 K)

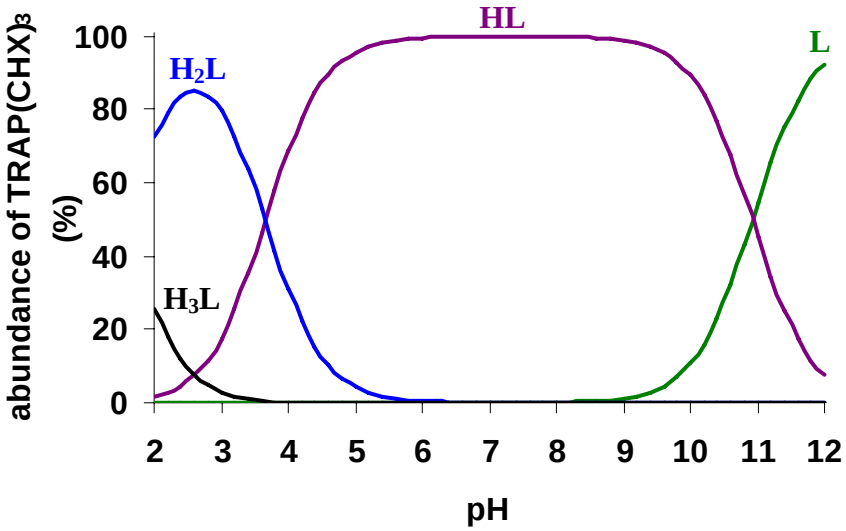

Figure A9. Species distribution of TRAP$(CHX)_3$ ([TRAP$(CHX)_3$]=2.0 mM, 0.15 M NaCl, 298 K)

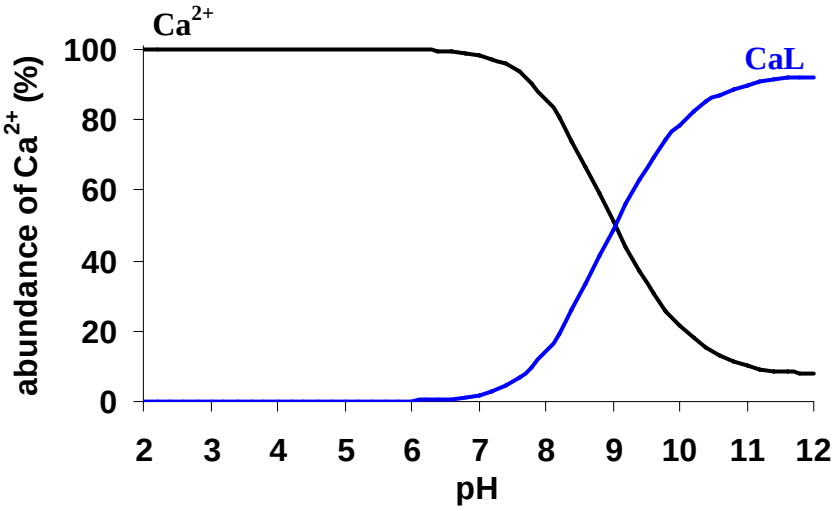

Figure A10. Species distribution of Ca^{2+} - TRAP(CHX)$_3$ system ([Ca^{2+}]=[TRAP(CHX)$_3$]=2.0 mM, 0.15 M NaCl, 298 K)

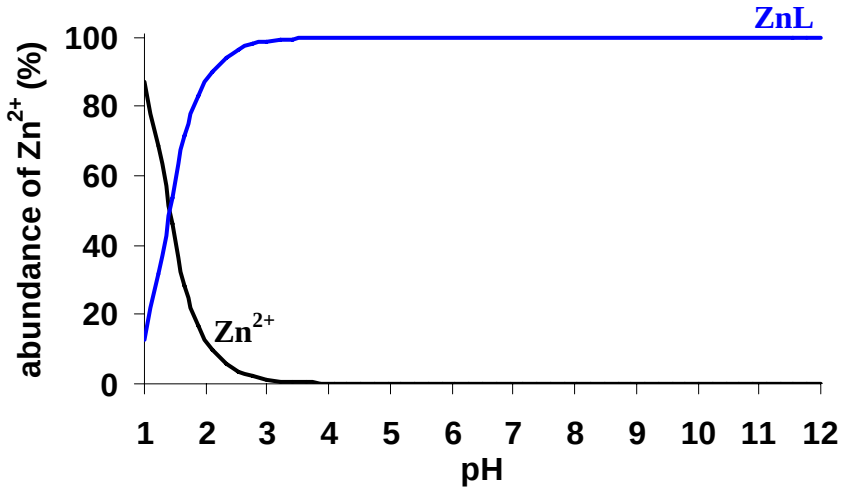

Figure A11. Species distribution of Zn^{2+} - TRAP(CHX)$_3$ system ([Zn^{2+}]=[TRAP(CHX)$_3$]=2.0 mM, 0.15 M NaCl, 298 K)

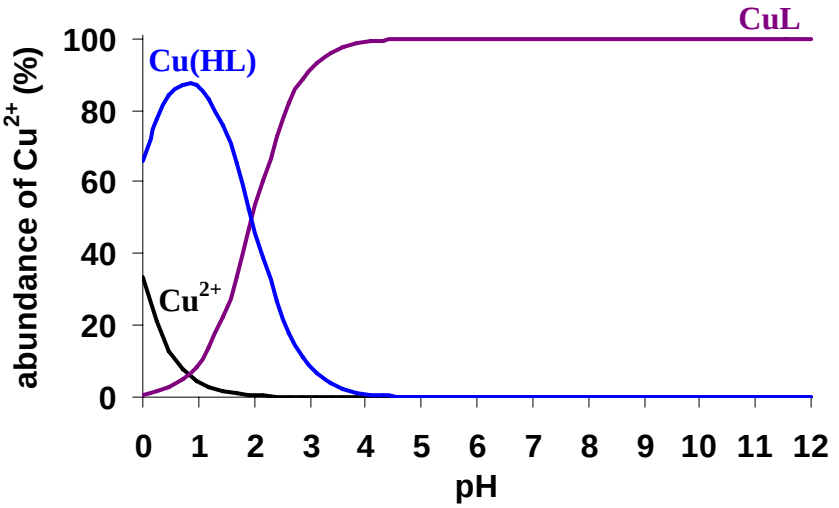

Figure A12. Species distribution of Cu^{2+} - TRAP(CHX)$_3$ system ([Zn^{2+}]=[TRAP(CHX)$_3$]=2.0 mM, 0.15 M NaCl, 298 K)

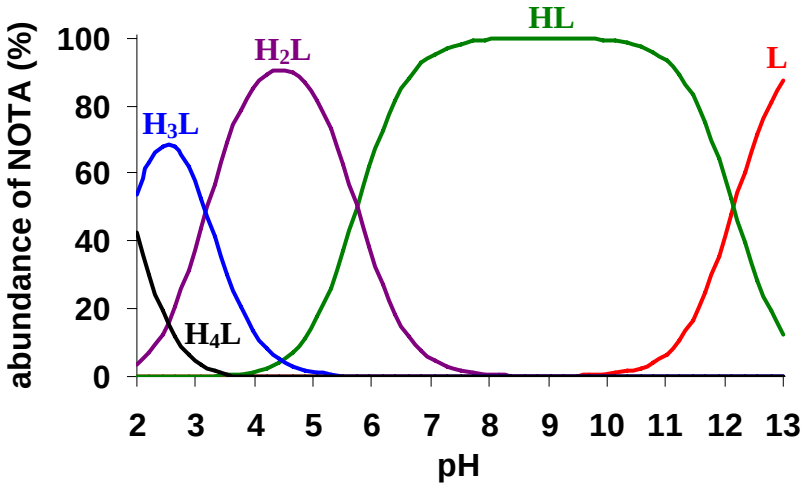

Figure A13. Species distribution of NOTA ([NOTA]=2.0 mM, 0.15 M NaCl, 298 K)

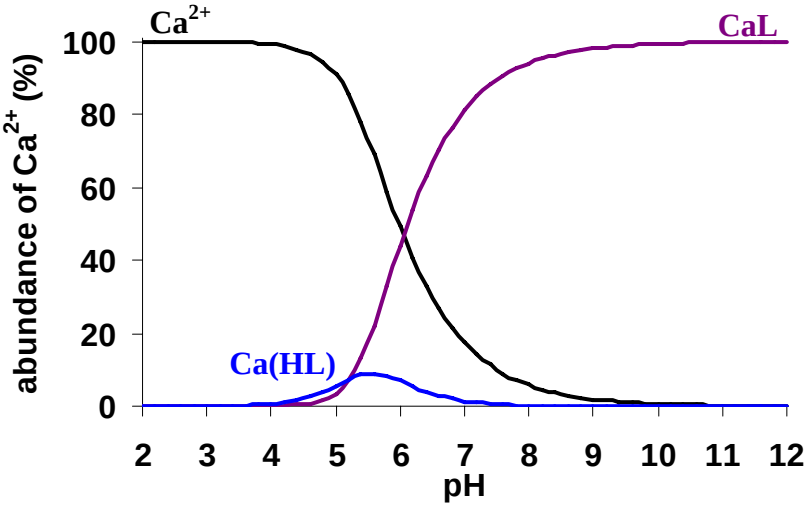

Figure A14. Species distribution of Ca^{2+} - NOTA system ([Ca^{2+}]=[NOTA]=2.0 mM, 0.15 M NaCl, 298 K)

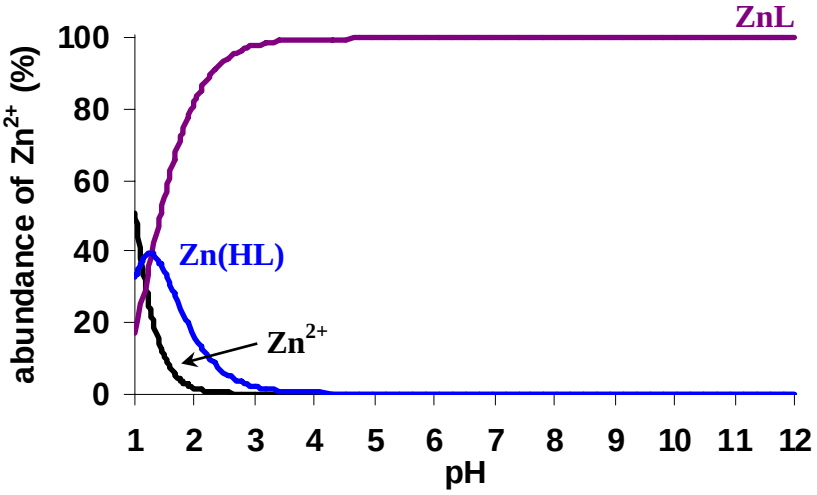

Figure A15. Species distribution of Zn^{2+} - NOTA system ([Zn^{2+}]=[NOTA]=2.0 mM, 0.15 M NaCl, 298 K)

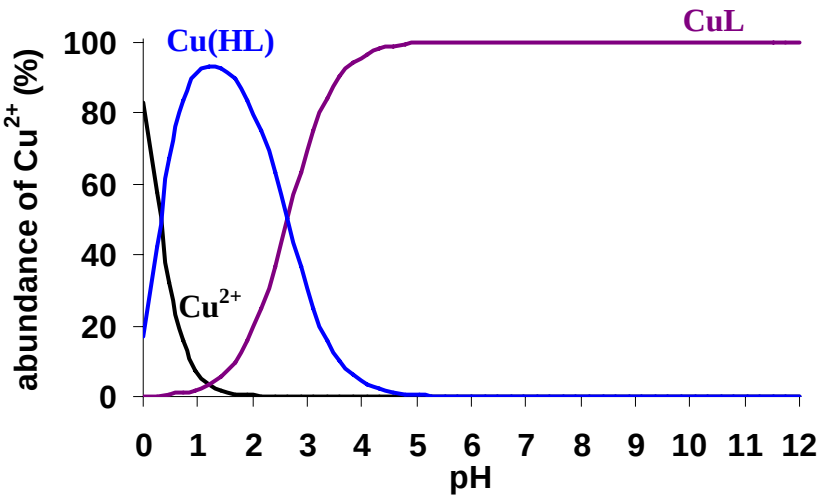

Figure A16. Species distribution of Cu^{+} - NOTA system ([Cu^{2+}]=[NOTA]=2.0 mM, 0.15 M NaCl, 298 K)

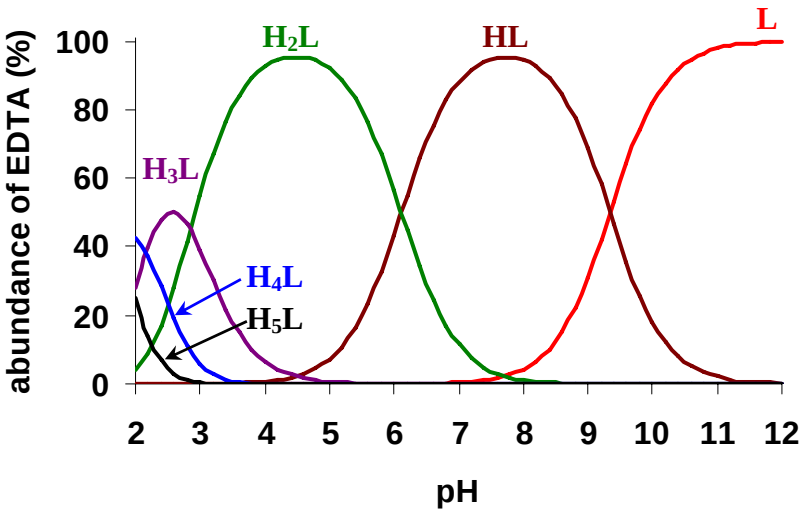

Figure A17. Species distribution of EDTA ([EDTA]=2.0 mM, 0.15 M NaCl, 298 K)

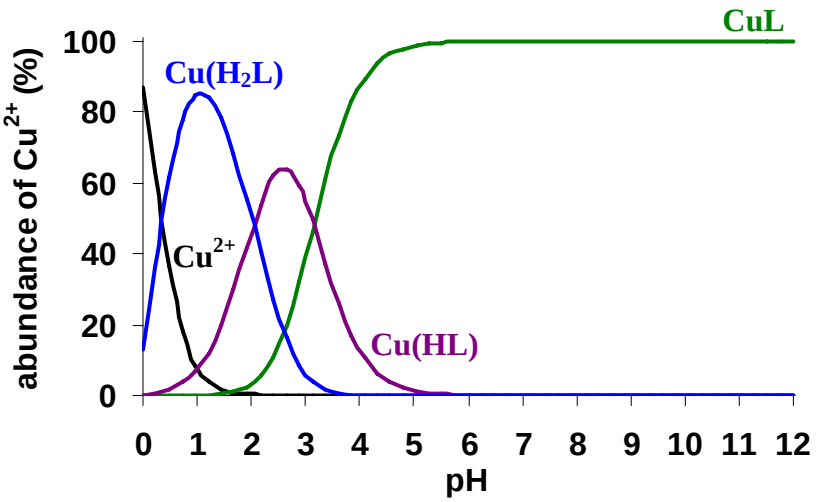

Figure A18. Species distribution of Cu^{+} - EDTA system ([Cu^{2+}]=[EDTA]=2.0 mM, 0.15 M NaCl, 298 K)